The Generation and Accumulation of Timing Noise in PCM Systems—An Experimental and Theoretical Study

By J. M. MANLEY

(Manuscript received September 30, 1967)

Three sources of timing noise in a self-timed regenerative PCM repeater, namely, tank circuit mistuning, amplitude to phase conversion, and pulse shape, were studied both experimentally and theoretically. We discuss how these noises accumulate and combine along a chain of repeaters.

The theoretical work is from the viewpoint of frequency analysis which leads easily to the spectrum of the timing noise. We first give a simple form of this theory applicable in a number of cases, and then a more general form useful in other cases, which shows the approximations and limitations of the simple theory.

We found that the spectrum of timing noise caused by tank circuit mistuning has no energy at zero frequency and because of this fact, timing noise from this source does not build up indefinitely along a chain of repeaters but soon reaches a limit. On the other hand, the spectrum of timing noise caused by amplitude to phase conversion does have energy at zero frequency; thus, timing noise from this source increases indefinitely along a repeater chain. Some of the timing noise is attributable to pulse shape alone and in some cases may include a very low frequency part. This latter comes about through the small energy near the harmonics of the pulse rate in the tuned circuit response and the aliasing of this energy down to very low frequencies by the sampling process used in measuring the phase deviation or in generating the retiming pulses.

I. INTRODUCTION AND SUMMARY

A considerable amount of work has been done and results published on the subject of timing noise in pulse code modulation (PCM) systems.[1–11] The material in this paper comes from work which began as

an experimental investigation. This led to some successful simple theories and generalizations along somewhat different lines from those followed previously.

It appears to be impossible for a regenerative repeater to perfectly restore a train of signal pulses to its original form because of the difficulty of obtaining a perfect timing source at a repeater location remote from the transmitter. The most widely used simple method of obtaining a timing wave is to pass the incoming pulse train, or some modification of it, through a narrowband resonant tank circuit, tuned as nearly as possible to the pulse rate. Since the tuning of the tank is unlikely to coincide with the pulse rate, since the bandwidth of this selective circuit is finite, and for other reasons, the derived timing wave is not perfect. Through this imperfect timing source, a certain amount of timing noise is added at each repeater to that already present in the incoming signal train.

Because this noise arises from imperfections in the system, it may be considered to be analogous to the modulation interference noise in amplitude systems caused by small departures from linearity in various components. Thus, if the narrowband tank circuit could be centered exactly on the pulse rate and kept there, and if the pulse generating circuits were always triggered exactly at a zero crossing of the timing wave, and if nonlinearity were not required to generate the pulse rate, then major sources of timing noise at a regenerative repeater would not exist.

As pointed out by W. R. Bennett and others, the principal effects of timing noise are two:[1]

(*i*) At any one repeater, the phase of the timing wave may be displaced in an irregular way from the proper place for optimum gating of signal pulses so that, at best, the tolerance of the system to noise is reduced and, at worst, errors in recognition of pulses or spaces are made.

(*ii*) Even if the sequence of pulses and spaces arrives at the receiver with no errors, the decoded signal samples will be irregularly spaced, thus introducing into the signal circuits a distortion which has the frequency of the deviation. The seriousness of this effect depends on its magnitude and the character of the signal. This effect is analyzed by W. R. Bennett in Ref. 1.

A program of measurements for studying the properties of this timing noise, and how it accumulates along a chain of regenerative

repeaters, was begun because of the difficulties which had been encountered in trying to calculate the noise. It was planned to isolate the sources of timing noise and so consider each one separately and then in combination. The work described here is not concerned with the effects of the noise on the system.

Measurements were not made on chains of varying numbers of real repeaters. Instead the chain is simulated by one real special repeater and a multitrack tape recorder as indicated by Fig. 1. While the previous repeater output is being reproduced from two tracks of the recorder and used as input for the real repeater, the new output is being recorded on two other tracks. One of each pair of tracks is used for the pulse train and the other for timing information. Because no recorder has steady enough speed, the timing wave cannot be recorded directly. Instead, the phase deviations are detected and these are recorded. During playback, the timing wave is reconstructed with a phase modulator. The recording is sufficiently long so that statistical fluctuations are well smoothed. For most of the work the pulse train consisted of random unipolar pulses at a 1 kHz rate.

The first results obtained were on the noise caused by mistuning of the timing tank in one repeater and then two in tandem. Study of these results led to the development of a simple theory for the gen-

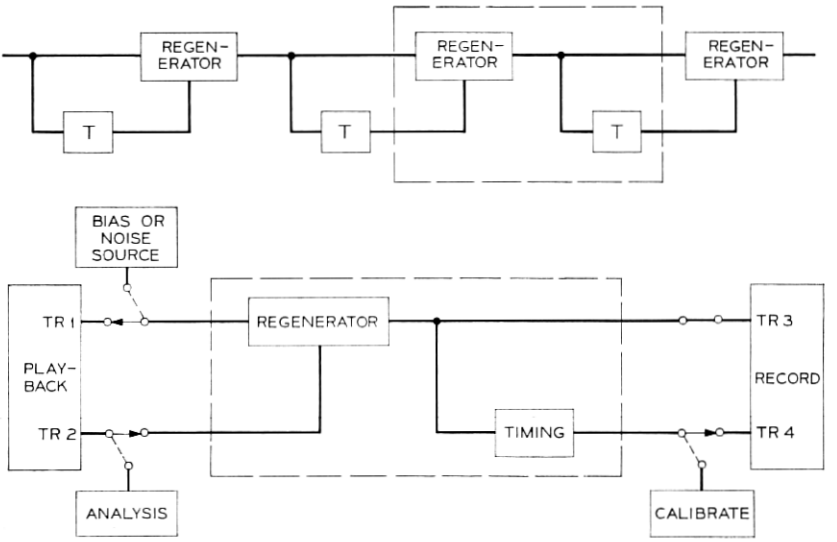

Fig. 1 — Simulation of regenerative repeater chain.

eration of the timing noise and its accumulation along a chain of repeaters. Subsequent work demonstrated that this theory may be used to calculate the noise satisfactorily, not only for longer chains, but for amplitude to phase conversion sources of timing noise as well. Very good agreement was obtained between the noise calculated from this theory and that measured.

A brief summary of these results obtained when narrow rectangular pulses are used follows:

The spectra of timing noise at each of the repeaters in a chain of six, all mistuned alike, are shown in Fig. 2. This noise is designated

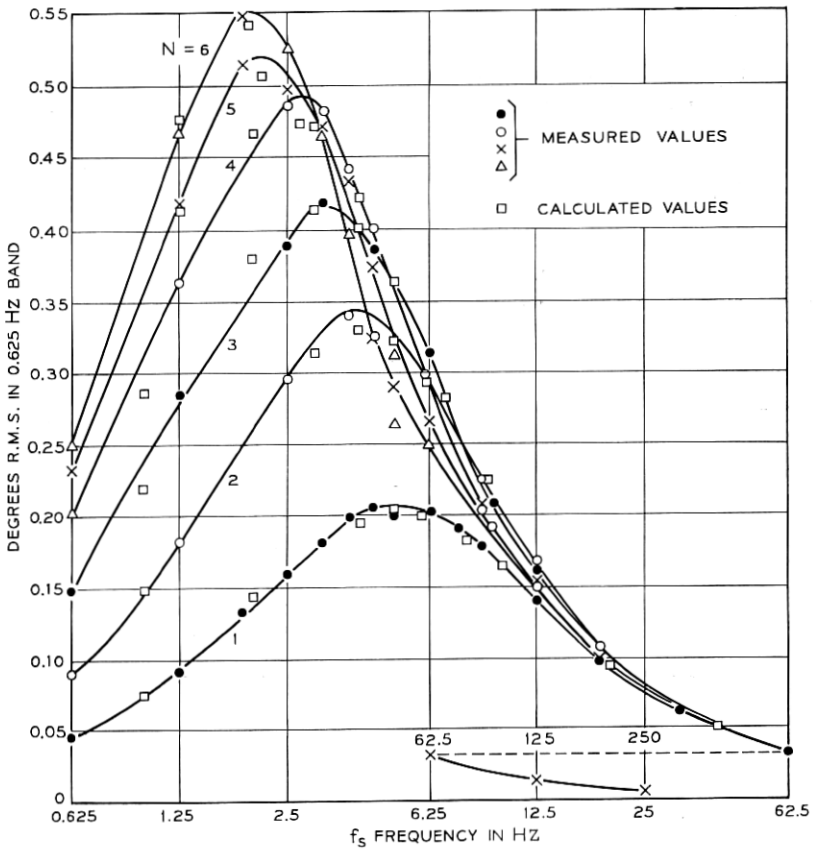

Fig. 2 — Spectra of timing noise caused by 0.1 percent mistuning of timing tank, $Q = 100$. Random rectangular pulses, 10 percent duty factor. N = number of like repeaters in chain.

Type *A*; the most important characteristic of these spectra is that there is no energy at zero frequency. Because of this, the peak of the spectrum at the end of a chain never becomes larger than four times the peak at the first repeater, no matter how long the chain is. The root mean square (rms) value of the total noise increases to about twice the amount at the first repeater as we go along a very long chain. If, as is most likely, some of the repeaters in the chain are mistuned in the opposite direction or to a smaller degree, the noise at the end is smaller than that above. Thus it is seen that mistuning of the timing tank is not a factor in the accumulation of large amounts of timing noise in a long chain of regenerative repeaters.

The situation is different, though, if we have a pulse generator whose trigger point is offset from a zero crossing. The timing noise in this case is a direct consequence of the amplitude variation of the timing wave, which variations have a spectrum with nonzero value at zero frequency. As shown in Fig. 3, this causes the rms value of very low frequency timing noise to increase linearly at successive repeaters in a chain having equally offset triggers in each. This noise is designated type *B*. The total noise at the end of the chain increases without limit as the number of repeaters increases. The total amount varies inversely as the Q of the tank circuits.

It was demonstrated that the theory applies also when both mistuning and amplitude-to-phase conversion are present simultaneously.

Spectra of timing noise caused by pulse shape alone are shown for several particular shapes in Fig. 4. While the total noise for the wider pulses is fairly large here, because it is spread over a wide frequency band, the magnitude of the undesirable very low frequency components is quite small. For example, the total noise for the asymmetrical overlapping pulses is only one-fifth the amount per repeater measured in the T1 system.[8] The results of this investigation indicate that some form of amplitude-to-phase conversion is probably the greatest source of very low-frequency timing noise.

The idea that, for the propagation of phase deviations, the chain of regenerative repeaters resembles a chain of tandem low-pass resistance-capacitance (RC) filters follows from considering the phase deviation to be a modulation of a carrier wave at the pulse rate. Experiments verified this idea which had been suggested earlier.[8]

A brief outline of the simple theory and method of calculation will now be given; a more detailed description will be made in Sections 2.1—2.5. Consider the spectrum of the incoming pulse train,

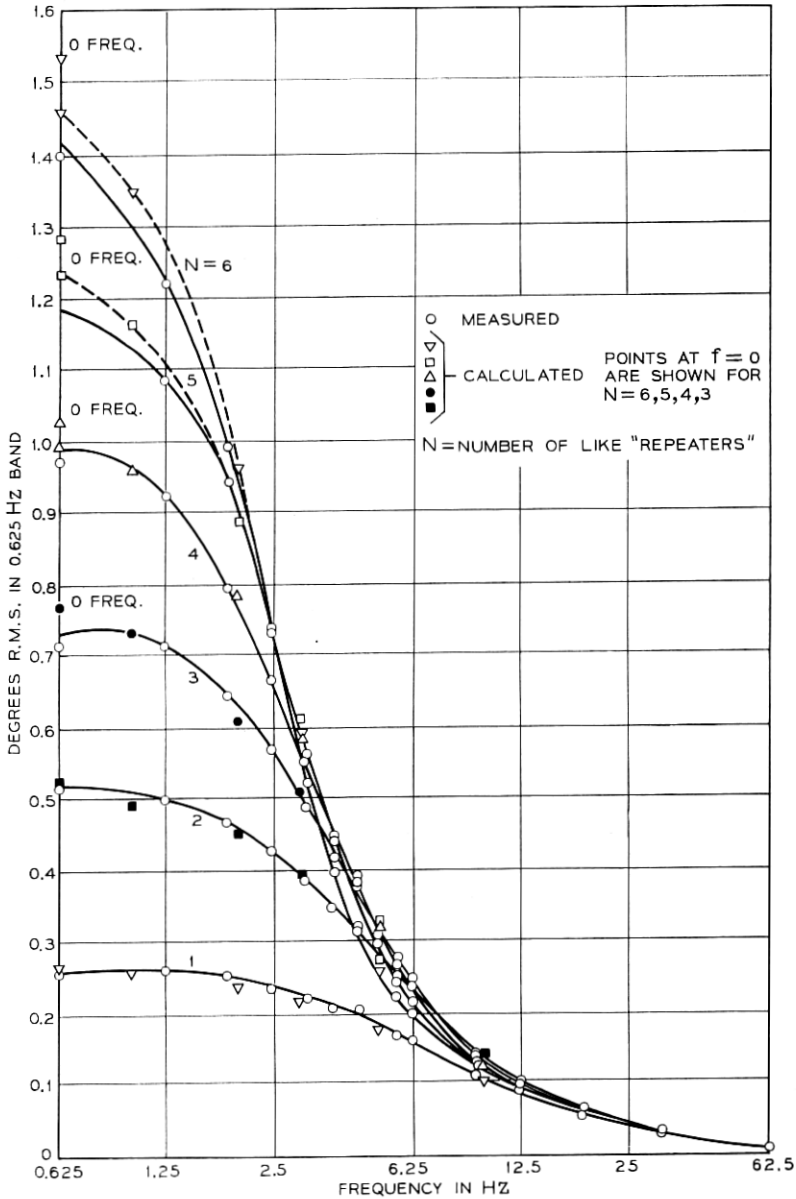

Fig. 3 — Spectra of timing noise caused by timing wave amplitude variations and trigger circuit offset from zero. Tank tuned to pulse rate. Random rectangular pulses, 10 percent duty factor. N = number of like repeaters in chain.

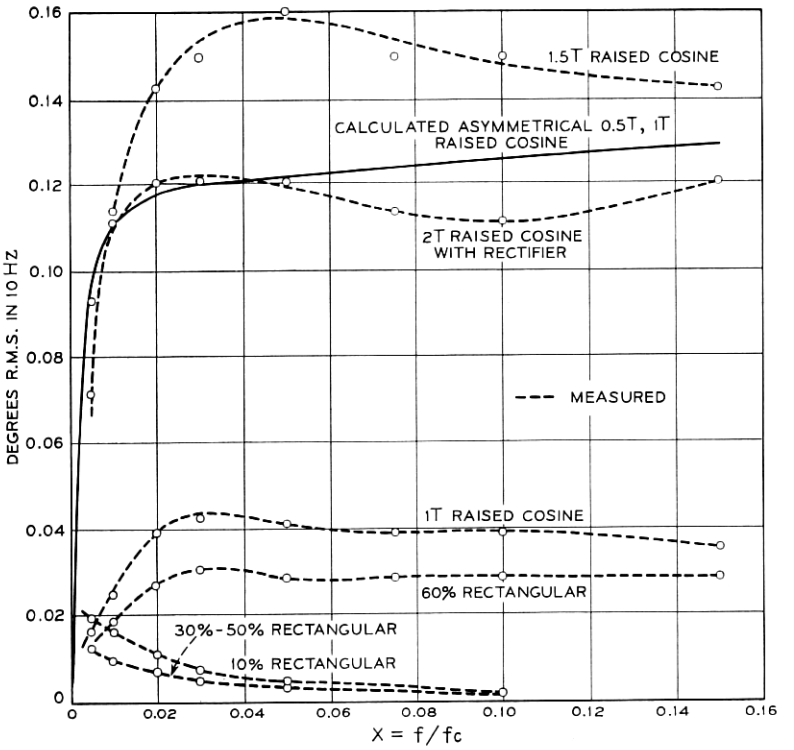

Fig. 4 — Timing noise spectra caused by various pulse shapes.

which will contribute very little timing noise itself if the pulses are narrow.* This spectrum consists of discrete components at harmonics of the pulse rate and a broadband of a special kind of noise.[1] Next consider this broadband of noise to be divided into small evenly spaced bands, each small band replaced by a single frequency component having the same power as the small band. Taking these side-frequencies in pairs about the pulse rate, we may think of the spectrum of the pulse train in the vicinity of the pulse rate as a carrier wave amplitude modulated by a number of small components.

The tuned circuit by which the pulse rate fundamental is selected from this spectrum to provide a timing wave, also admits some of the noise side frequencies which are still symmetrical if the tuned circuit is centered exactly on the pulse rate. When this tank circuit is

* The meaning of this is brought out in Sections 4.3, 2.6.5, and 2.6.6.

detuned from the pulse rate, the side-frequency pairs in the tank response are no longer symmetrical about the carrier. Sometimes the dissymmetry is described by saying that a quadrature carrier term has been introduced. The dissymmetry in amplitude, or phase, or both, is equivalent to phase modulation of the timing wave. This phase modulation of the timing wave is transferred to the outgoing pulse train in the regeneration process.

Next, assume that these asymmetrical side frequencies (which are another description of the above phase modulation), after being attenuated and phase shifted in transmission through the narrowband tank of the second repeater, would add directly to the corresponding ones newly generated by the detuning of the second tank. Phase deviation calculated from this assumption agrees very closely with that measured, not only after two repeaters, but after many have been traversed.

If the amplitude modulation at the tank output, corresponding to the symmetrical components, is not entirely removed by a limiter, that remaining may cause further phase modulation. For example, if a pulse generating circuit is supposed to trigger at a zero crossing of the timing wave but actually triggers a few degrees away from zero, amplitude variations of the timing wave will be converted to phase variations. The magnitude of these phase variations and their increase along a chain of repeaters may be successfully calculated using the same methods described above.

The simple theory applicable in a number of cases, and which leads easily to the spectrum of timing noise, is inadequate for pulse shapes other than narrow ones. Here the pulse train itself is now a source of timing noise. For example, if the pulses have a finite width, a small additional amount of noise (type *B*) can arise, although not in all cases. The limitations of the simple theory and how it fits into a more general theory is discussed in detail in Section 2.6.

The more general theory, described in Section 2.6, is also developed from a frequency viewpoint and is based on analysis by S. O. Rice to whom I am indebted for this work. With it the amount of timing noise in the situations of the previous paragraph were calculated. Also, this theory was used to calculate the timing noise for raised cosine pulses two time slots wide, hence with large enough overlapping so that a non-linear device is required in order to derive the pulse rate fundamental. It was found that in this case, the timing noise is Type *A* (that is, it does not build up in a long chain of repeaters) with a small qualification discussed in Section 2.6.6.

Another source of type B noise (which builds up indefinitely) is in any low-frequency distortion of the pulse spectrum if this is followed by a nonlinear operation of any kind.

II. THEORY OF PHASE NOISE GENERATION AND ACCUMULATION

As mentioned in the Section I, the simple theory is described first, with the more general one and its relation to the simple one being discussed in Section 2.6. The principal area in which the simple theory is satisfactory is that in which the pulses are narrow. In this case the pulse train itself causes very little timing noise, and so other sources may be considered separately.

2.1 *Spectrum of Narrow Pulse Train*

It is assumed that the message pulses are represented by a random train of narrow, rectangular, unipolar pulses. By random pulse train is meant one having regularly spaced pulse positions which are filled or not at random. Although most of the work was done for an average pulse density of one-half, the result would not be appreciably different except in magnitude, if this parameter differed somewhat from the value one-half.

The spectrum of this train has been calculated by W. R. Bennett.[1] Part of the spectrum is a series of harmonics, the fundamental of which is the pulse rate, and the magnitudes of which are determined by the shape of the individual unit pulses. The spectrum of the other part has the same shape as the envelope of harmonics, and is continuous and therefore is a noise. Bennett points out that while this noise is like thermal noise in some respects, that is, for example, in the proper frequency band the two sound alike; nevertheless it has a phase structure which thermal noise does not.

If the original pulses are rectangular of height V_o and duration τ and occur at regular intervals $T = 1/f_c$ with a probability of 1/2, Bennett's calculation shows that the mean square value of the fundamenal term at $f = f_c$ is

$$A_1^2/2 = (V_o^2/2\pi^2) \sin^2 \pi\tau/T \tag{1}$$

and that the mean square value (in a band B Hz wide) of the noise part is

$$W(f) = B(V_o^2/2\pi^2)(f_c/f^2) \sin^2 (\pi\tau f). \tag{2}$$

From a somewhat different point of view, the spectrum of this

random train of narrow pulses may be calculated by first considering the train to consist of repeated blocks of random pulses, each block being N pulse periods T in length. The Fourier series representation of this train consists of harmonics of the pulse rate f_c plus single frequency "noise" components spaced f_c/N apart. The harmonics have nonzero average values. While the noise components have zero average values, their average powers are nonzero. If N is made to approach infinity, this spectrum approaches that calculated by Bennett. The representation by finite components means, in effect, that a band of noise f_c/N Hz wide is replaced by a discrete term having the same mean square value. If S and A_i are the rms amplitudes of one of the noise components and the pulse rate fundamental, respectively, then, as shown in (113), Section 2.6.5,

$$S^2/A_i^2 = \frac{(Bf_c)\sin^2(\pi f\tau)}{f^2\sin^2(\pi\tau f_c)}, \tag{3}$$

where f_c/N has been replaced by B. This agrees with (1) and (2) from Bennett's calculation. In the vicinity of the fundamental, we have

$$S/A_i \approx (B/f_c)^{\frac{1}{2}}.$$

The spectrum of this representation of the pulse train is shown in Fig. 5.

Near the pulse rate component, the noise amplitudes on both sides of it are nearly equal because the pulses are narrow. For example, when $\tau/T = 0.1$, values of S for components 2.5 percent above and below f_c differ by about 0.2 percent. Hence an approximate representation of this region of the spectrum is

$$E_i = A_i[1 + \sum a_k \cos(2\pi k f_c t/N)]\cos 2\pi f_c t \tag{4}$$

where

$$a_k = 2S/A_i \approx 2(B/f_c)^{\frac{1}{2}} \tag{5}$$

which describes the input as an amplitude modulated carrier. A more accurate representation would include a modulated quadrature term to account for the slight dissymmetry of side frequencies.

It is the regular spacing of the random pulses which gives the phase structure to the noise spectrum, causes zeros of the wave E_i to appear at regular intervals $T = 1/f_c$ apart, and which makes possible the representation in (4).

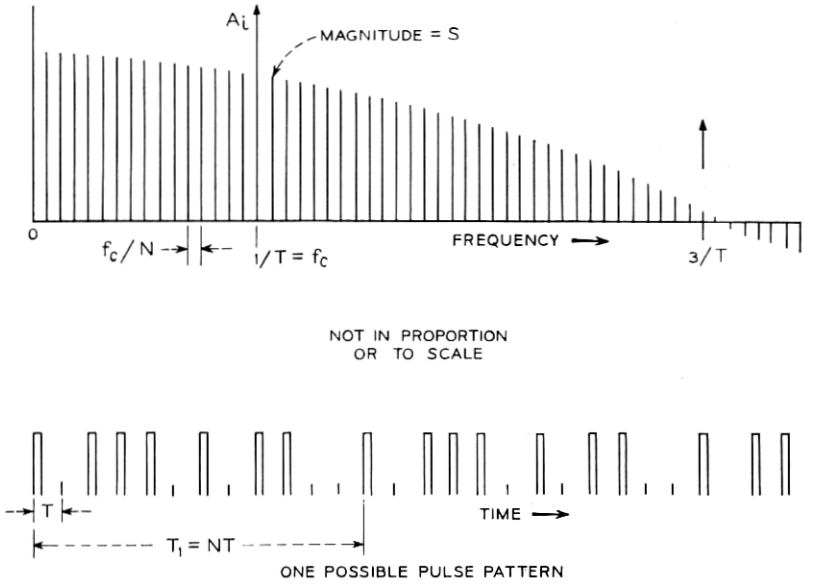

Fig. 5 — Pulse pattern and spectrum.

In the simple theory, attention is given only to that part of the pulse spectrum in the vicinity of the pulse rate fundamental as indicated by the representation (4). The strength of the noise terms with respect to the fundamental is obtained by the indicated statistical averaging of the pulse train components with the result (3). The reasons why these simplifications are satisfactory are discussed in Section 2.6.

In the Section 2.2, the response of the tuned circuit to this restricted portion of the pulse spectrum, considering the noise terms to have fixed amplitudes, is calculated.

2.2 *Response of Tuned Circuit to Narrow Pulses*

In calculating the response of the tuned circuit to (4), we need to consider only one representative modulation term of frequency $q/2\pi = kf_c/N$, namely

$$E_{ik} = A_i[1 + 2(S/A_i) \cos qt] \cos \omega_c t. \tag{6}$$

The response to the two side frequencies $S \cos (\omega_c \pm q)t$ of this one term is

$$E_{os} = S_1 \cos(\omega_c t + qt + \theta_1) + S_2 \cos(\omega_c t - qt + \theta_2)$$
$$= S_1 \cos[(\omega_c t + \varphi) + qt + (\theta_1 - \varphi)] + S_2 \cos[\omega_c t + \varphi) - qt - (\varphi - \theta_2)], \quad (7)$$

where θ_1 and θ_2 and φ are the phase shifts received by the two side frequencies and the carrier respectively in going through the tuned circuit. If the tuned circuit is resonant at ω_c, the symmetry of the side frequencies about ω_c in both amplitude and phase which exists in (4) is preserved in the response. But if it is resonant at ω_o, different from ω_c, the response side frequencies are unsymmetrical as indicated in Fig. 6. In this case, they may be resolved into a pair with even symmetry and a pair with odd symmetry, or into a component in phase with the carrier and another in quadrature with the carrier. That is, we get

$$E_{os} = A_s \cos[\omega_c t + \varphi + qt + \varphi_s] + A_s \cos[\omega_c t + \varphi - qt - \varphi_s] + A_a \cos[\omega_c t + \varphi + qt + \varphi_a] - A_a \cos[\omega_c t + \varphi - qt - \varphi_a]$$
$$= 2A_s \cos(qt + \varphi_s) \cos(\omega_c t + \varphi) - 2A_a \sin(qt + \varphi_a) \sin(\omega_c t + \varphi) \quad (8)$$

where

$$2A_s = \{S_1^2 + S_2^2 + 2S_1S_2 \cos[(\varphi - \theta_2) - (\theta_1 - \varphi)]\}^{\frac{1}{2}}$$
$$2A_a = \{S_1^2 + S_2^2 - 2S_1S_2 \cos[(\varphi - \theta_2) - (\theta_1 - \varphi)]\}^{\frac{1}{2}} \quad (9)$$
$$\tan \varphi_s = \frac{S_1 \sin(\theta_1 - \varphi) + S_2 \sin(\varphi - \theta_2)}{S_1 \cos(\theta_1 - \varphi) + S_2 \cos(\varphi - \theta_2)}$$
$$\tan \varphi_a = \frac{S_2 \sin(\varphi - \theta_2) - S_1 \sin(\theta_1 - \varphi)}{S_2 \cos(\varphi - \theta_2) - S_1 \cos(\theta_1 - \varphi)}.$$

Thus the resonant tank response to the amplitude modulated wave (6) is

$$E_o = [A_o + 2A_s \cos(qt + \varphi_s)] \cos(\omega_c t + \varphi) - [2A_a \sin(qt + \varphi_a)] \sin(\omega_c t + \varphi). \quad (10)$$

When S/A_i is small, as at present, (10) is approximately described by

$$E_o \approx A_o[1 + 2(A_s/A_o) \cos(qt + \varphi_s)] \cos[(\omega_c t + \varphi) + 2(A_a/A_o) \sin(qt + \varphi_a)]. \quad (11)$$

The tuned circuit to which the train of random pulses is applied

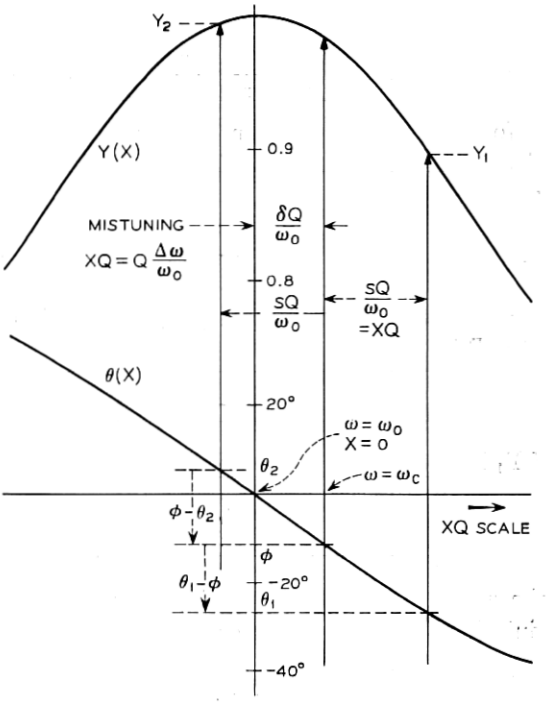

Fig. 6 — Resonant circuit characteristics.

in order that the pulse rate fundamental may be selected is described by

$$\frac{I}{E} = Y(j2\pi f) = \frac{1}{R + j\left(\omega L - \frac{1}{\omega C}\right)}. \tag{12}$$

Let

$$\begin{aligned} \omega_o^2 LC &= 1 \\ \omega_o L/R &= Q \\ \omega &= n\omega_o + \Delta\omega \\ \Delta\omega/\omega_o &= x. \end{aligned} \tag{13}$$

Then

$$Y(j2\pi f_o) = \frac{1}{R} \tag{14}$$

and

$$Y(j2\pi f)/Y(j2\pi f_o) = \frac{n + x}{n + x + jQ[(n + x)^2 - 1]}. \tag{15}$$

This general formula will be used in the treatment for wide pulses. Here we will be concerned only with frequencies in the neighborhood of f_o and so we set $n = 1$. Thus

$$Y_1(j2\pi f)/Y(j2\pi f_o) = \frac{1 + x}{1 + x + j2Qx(1 + x/2)}. \tag{16}$$

When $\Delta\omega/\omega_o = x$ is small, a satisfactory approximation to the transmission $Y_1(j2\pi f)R$ is

$$Y_1(j2\pi f)R \approx \frac{1}{1 + j2Q\ \Delta\omega/\omega_o}. \tag{17}$$

The phase of Y_1 is θ, where $\tan\theta = -2Q\Delta\omega/\omega_o$. Let

$$\begin{aligned} x_o &= \delta/\omega_o, & x_q &= q/\omega_o, \\ x_1 &= x_o + x_q, & x_2 &= x_o - x_q, \end{aligned} \tag{18}$$

where δ is the amount of tank circuit detuning from the carrier and q is the modulation frequency. It is convenient also to write

$$\begin{aligned} S_1/S &= |\ Y[j2\pi f_o(1 + x_o + x_q)]\ |\ R = y_1 = \cos\theta_1 \\ S_2/S &= |\ Y[j2\pi f_o(1 + x_o - x_q)]\ |\ R = y_2 = \cos\theta_2. \end{aligned} \tag{19}$$

The amounts of amplitude and phase modulation in the tank circuit response (11) can now be given explicitly. Writing

$$\frac{2A_s}{A_o} = \left(\frac{S}{A_i}\right)\left(\frac{A_i}{A_o}\right)\left(\frac{2A_s}{S}\right),$$

then substituting (5) for the first ratio on the right, and the upper of (9) for the third ratio, and noticing that

$$A_o/A_i = |\ Y[j2\pi f_o(1 + x_o)]\ |\ R,$$

we have

$$\begin{aligned} 2A_s/A_o &= (B/f_c)^{\frac{1}{2}}(1 + \tan^2\varphi)^{\frac{1}{2}} \\ &\quad \cdot\{y_1^2 + y_2^2 + 2y_1y_2\cos[(\varphi - \theta_2) - (\theta_1 - \varphi)]\}^{\frac{1}{2}} \end{aligned} \tag{20}$$

Similarly,

$$\begin{aligned} 2A_a/A_o &= (S/A_i)(A_i/A_o)(2A_a/S) = (B/f_c)^{\frac{1}{2}}(1 + \tan^2\varphi)^{\frac{1}{2}} \\ &\quad \cdot\{y_1^2 + y_2^2 - 2y_1y_2\cos[(\varphi - \theta_2) - (\theta_1 - \varphi)]\}^{\frac{1}{2}}. \end{aligned} \tag{21}$$

When the amount of detuning is small (0.1 percent detuning with $Q = 100$ makes $\tan \varphi = 0.2$), the expression inside the large radicals of (20) and (21) may be simplified so that

$$2A_a/A_o \approx \frac{2(B/f_c)^{\frac{1}{2}}}{[1 + (2qQ/\omega_o)^2]^{\frac{1}{2}}} \tag{22}$$

$$2A_a/A_o \approx \frac{8(B/f_c)^{\frac{1}{2}}(\delta Q/\omega_o)(qQ/\omega_o)}{1 + (2qQ/\omega_o)^2}, \tag{23}$$

and also $\varphi_a \approx \theta$.

The two expressions in (22) and (23) describe the amplitudes of the amplitude and phase modulation in (11) which are the responses of the resonant tank circuit to an amplitude modulated wave representing part of the incoming pulse train. Before discussing the meaning of these results for the generation of phase modulation or how it accumulates in a chain of repeaters, we will calculate the amount of phase deviation generated by another possible source within the repeater.

2.3 *Amplitude to Phase Conversion Factor of Offset Trigger*

In an ideal repeater, a perfect limiter following the resonant tank circuit would remove all the amplitude modulation from the derived timing wave (11) which would then, at one of its zero crossings, trigger a pulse generator as a part of the retiming process. But in a real repeater, the limiting would not be perfect so that some amplitude modulation remains on the timing wave; also the trigger point may have drifted away from the zero crossing. This is one way in which amplitude variations of the timing wave are converted to phase variations in a regenerative repeater. The diagram of Fig. 7 illustrates the conversion.

Referring to Fig. 7, where the triggering level has been offset by the bias b or by the angle γ_o which are related by

$$\sin \gamma_o = b/A_o, \tag{24}$$

it is seen that the change, $\Delta\gamma$, in triggering angle for a change, ΔA, in amplitude is

$$\Delta\gamma = -\tan \gamma_o(\Delta A/A_o). \tag{25}$$

The amplitude variation in (11) at the tank circuit output is reduced by a factor K_L in the limiter which follows, so that the input

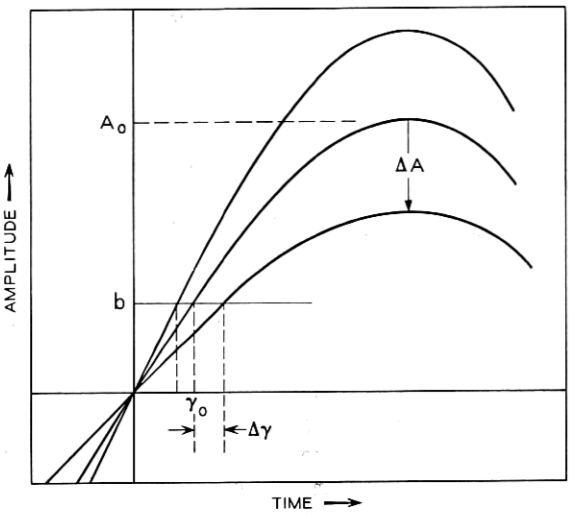

Fig. 7 — Amplitude-to-phase conversion in trigger with offset bias.

for the pulse generator is

$$A_o[1 + K_L(2A_s/A_o)\cos(qt + \varphi_s)]\cos[(\omega_c t + \varphi) + (2A_a/A_o)\sin(qt + \varphi_a)]. \quad (26)$$

Hence the phase variation introduced by the offset trigger, using $K_L 2A_s/A_o$ from (22) for $\Delta A/A_o$, is

$$\Delta\gamma = \frac{-2(B/f_c)^{\frac{1}{2}}K_L \tan\gamma_o}{[1 + (2qQ/\omega_o)^2]^{\frac{1}{2}}}\cos(q_t + \varphi_s). \quad (27)$$

2.4 *Application of These Results to Timing Noise*

The phase variations (referred to the carrier fundamental) of the pulse generator driven by (26) are then given by the sum of $\Delta\gamma$ from (27) and $2(A_a/A_o)\sin(qt + \varphi_a)$ from (23), that is,

$$\varphi_1 = \frac{8(B/f_c)^{\frac{1}{2}}(\delta Q/\omega_o)(qQ/\omega_o)}{1 + (2qQ/\omega_o)^2}\sin(qt + \varphi_a) - \frac{2(B/f_c)^{\frac{1}{2}}K_L \tan\gamma_o}{[1 + (2qQ/\omega_o)^2]^{\frac{1}{2}}}\cos(qt + \varphi_s) \quad \text{(radians)}. \quad (28)$$

From the magnitudes of the two components of (28), the spectra of timing noise caused by tank circuit mistuning and by amplitude to

phase conversion are determined. These are plotted in Fig. 8 with $K_L \tan \gamma_o = 1$. The phases φ_a and φ_s are plotted in Fig. 9. The first term in (28) specifies the spectrum if mistuning alone is present; the second term applies if mistuning is zero and there is amplitude to phase conversion. It is seen that the spectra in these cases are quite different at very low frequencies near $q = 0$. The phase modulation for mistuning alone is zero at zero frequency and has a maximum

$$\max (2A_a/A_o) = 2(B/f_c)^{\frac{1}{2}}(\delta Q/\omega_o) \tag{29}$$

at

$$2qQ/\omega_o = 1, \tag{30}$$

while that for amplitude to phase conversion alone has a maximum value of $2(B/f_c)^{\frac{1}{2}}K_L \tan \gamma_o$ at zero frequency. This difference between the two spectra at low frequencies has a very important effect on the accumulation of timing noise in chains of repeaters, as will be seen in Section 2.5. Second, we see that the first component depends directly on the amount of detuning, δ, and is zero for zero detuning. See Section 4.1. This emphasizes what Bennett has said about the difference between the noise spectra of random pulses and thermal noise.[1] In the latter case, phase noise would not be zero for zero detuning.

The good agreement between phase deviations calculated in this

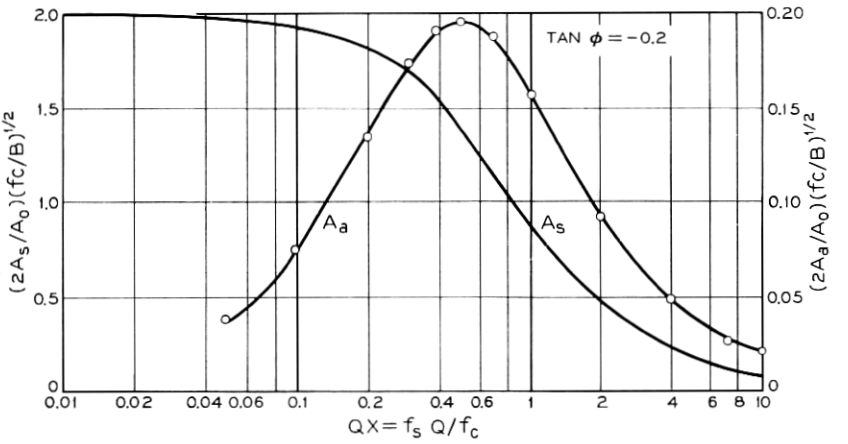

Fig. 8 — Amplitude spectra of symmetrical (A_s/A) and antisymmetrical (A_a/A) side frequencies caused by tank mistuning (calculated).

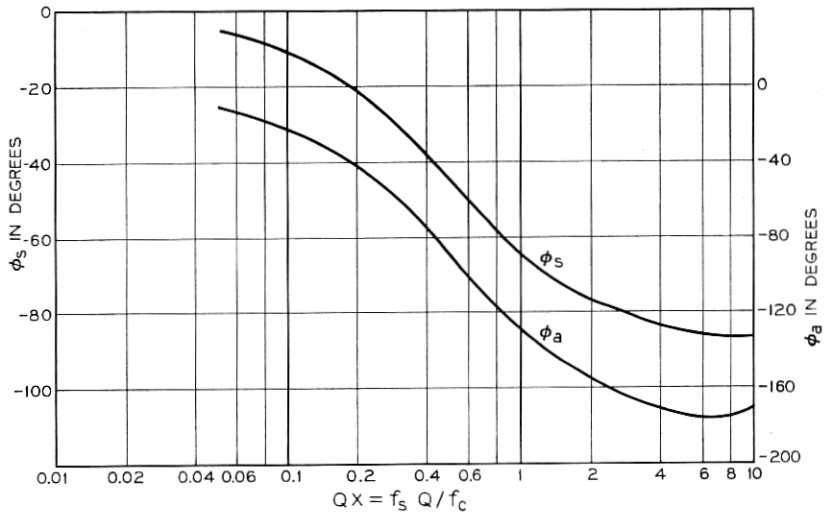

Fig. 9 — Phase spectra of symmetrical (Φ_s) and antisymmetrical (Φ_a) side frequencies caused by tank mistuning (calculated).

way, and measured values, has already been mentioned in the introduction and is shown in the curves of Fig. 2 and 3.

In one sense both of these effects are amplitude-to-phase conversion with the amplitude modulated carrier representation of part of the pulse train, as in (4), being the original amplitude variation. From this viewpoint, in both (23) and (27),

$$2(B/f_c)^{\frac{1}{2}}$$

is the applied amplitude variation; the factor

$$[1 + (2qQ/\omega_o)^2]^{\frac{1}{2}}$$

is the attenuation of the tuned circuit; while

$$-K_L \tan \gamma_o$$

is the amplitude-to-phase conversion factor in (27), and

$$\frac{4(\delta Q/\omega_o)(qQ/\omega_o)}{[1 + (2qQ/\omega_o)^2]^{\frac{1}{2}}}$$

is the corresponding conversion factor for mistuning from (23).

When both tank mistuning and trigger offset are present in the timing wave path, their combined effect may be calculated by adding

the two as suggested in (28). The correctness of this has been verified by experiment as seen in Fig. 10 where both measured data and values calculated according to (28) are plotted. This result emphasizes again that both of these phase modulation effects have a common source in the special noise side frequencies about the pulse rate in the spectral representation of the random pulse train.

2.5 *Accumulation of Phase Modulation in a Chain of Repeaters*

Next consider how phase modulation accumulates in a chain of repeaters when the same amount and kind of phase modulation is generated at each repeater of the chain.

Assume that phase modulation generated in the derived timing wave at repeater 1 is

$$\varphi_1 = \Phi_1 \sin (qt + \varphi_a) \tag{31}$$

and that this is passed along unchanged by the regenerator. Then at the input to repeater 2, this is equivalent to the presence of a pair

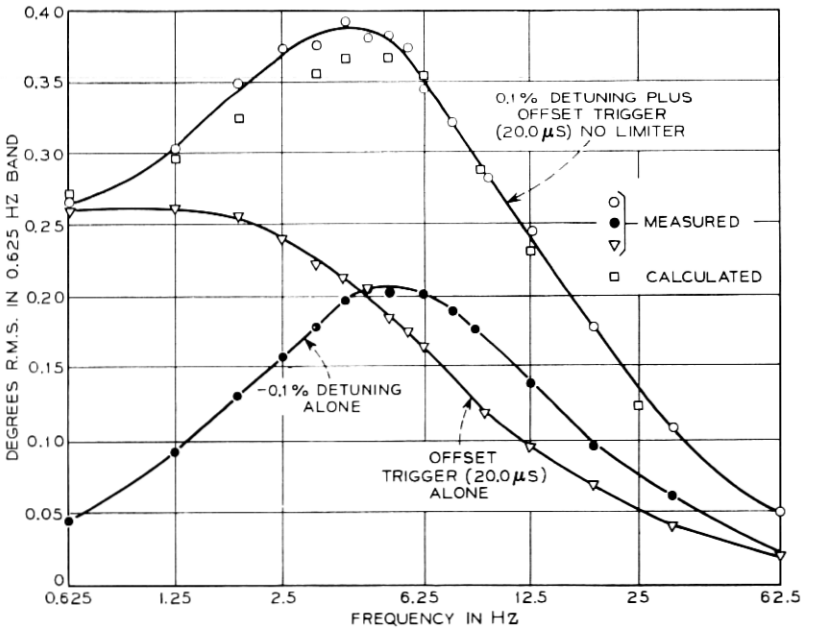

Fig. 10 — Spectrum of timing noise caused by tank detuning and trigger offset.

of antisymmetrical side frequencies

$$S_{\pm}/A = \pm(\Phi_1/2) \cos (\omega_c t + \varphi \pm qt \pm \varphi_a) \tag{32}$$

about the carrier. The transmission of these side frequencies through the tuned circuit of repeater 2 is governed by expressions (11), (20), and (22), developed above for the transmission of amplitude modulation. In using these in the present circumstance, the amplitude $\Phi_1/2$ in (32) takes the place of S/A_i in (20). The response of the tank circuit of repeater 2 to these side frequencies is then approximately

$$\pm \frac{\Phi_1/2}{[1 + (2qQ/\omega_o)^2]^{\frac{1}{2}}} \cos (\omega_c t + \varphi \pm qt \pm \varphi_a \pm \varphi_s) \tag{33}$$

if it is assumed that the pulse amplitude, and hence that of the carrier, are the same at repeater 2 as at repeater 1. This expression is independent of mistuning when the degree of mistuning is small, as we have assumed. In addition to this response we have the pair of antisymmetrical side frequencies, as expressed by (32), but now generated at repeater 2, namely

$$\pm (\Phi_1/2) \cos (\omega_c t + \varphi \pm qt \pm \varphi_a). \tag{34}$$

Thus at the output of the tank circuit of repeater 2, the antisymmetrical side frequencies are represented by the sum of these two, that is (34) and (33) or,

$$\pm(\Phi_1/2)\Big\{\cos (\omega_c t + \varphi \pm qt \pm \varphi_a) + \frac{1}{[1 + (2qQ/\omega_o)^2]^{\frac{1}{2}}} \cos (\omega_c t + \varphi \pm qt \pm \varphi_a \pm \varphi_s)\Big\}.$$

Therefore the total modulation Φ_2 at the output of repeater 2 is seen to be

$$\Phi_2 = | \Phi_1 + \Phi_1 (\cos \theta) \exp (j\theta) | \tag{35}$$

where $\cos \theta$ has been substituted for

$$\frac{1}{[1 + (2qQ/\omega_o)^2]^{\frac{1}{2}}}$$

according to (19), and φ_s has been replaced by its approximation θ. Carrying through the same process for repeater 3, we find the phase modulation at repeater 3 output to be

$$\Phi_3 = \Phi_1 | 1 + (\cos \theta) \exp (j\theta) + (\cos \theta)^2 \exp (j2\theta) |. \tag{36}$$

These show that, while the actual combining process at each repeater involves the direct addition of side frequencies, we can drop the carrier reference and consider the generation and propagation of modulation alone. And the Φ_1 generated at each repeater need not be only the component (23), but may be the more general one (28) in which mistuning and amplitude to phase conversion effects are combined.

The process begun in (36) may be generalized to give the amount of phase noise at the Nth repeater in a chain of N-like repeaters. This is

$$\Phi_N = \Phi_1 \mid (Y)_N \mid = \Phi_1 \left| \sum_{n=0}^{N-1} (Y_1R)^n \right| = \Phi_1 \left| \frac{1 - (Y_1R)^N}{1 - Y_1R} \right|, \tag{37}$$

where Y_1R has been written for (16). The approximation (17) to Y_1R and the relation (19) are used so that

$$Y_1R \approx \frac{1}{1 + j2x_qQ} = (\cos\theta) \exp(j\theta), \tag{38}$$

where $x_q = q/\omega_o$ as defined in (18). In (37), $(Y)_N$ is not an admittance as Y_1 is, but is a transfer function. By direct expansion of $(Y)_N$, using (38),

$$\mid (Y)_N \mid^2 = \frac{1 + (\cos\theta)^{2N} - 2(\cos\theta)^N \cos N\theta}{\sin^2\theta}. \tag{39}$$

$(Y)_N$ may be considered a sort of phase deviation transfer function for a chain of N repeaters when Φ_1 is the phase deviation generated in each repeater. $|(Y)_N|$ is plotted for $N = 4, 30, 100$ in Figs. 11, 12, and 13.

Since Φ_1 and $(Y)_N$ are functions of the phase deviation frequency q, $|\Phi_N|$ will describe the spectrum of accumulated phase noise. Consider first the case of tank circuit mistuning alone. From (23), we have

$$\Phi_1 = K_1 \frac{4x_qQ}{1 + (2x_qQ)^2} = 2K_1 \sin\theta \cos\theta \quad \text{(radians)} \tag{40}$$

where

$$K_1 = 2(B/f_c)^{\frac{1}{2}}(\delta Q/\omega_o). \tag{41}$$

Then for mistuning,

$$\mid \Phi_N \mid^2 = 4K_1^2 \cos^2\theta[1 + (\cos\theta)^{2N} - 2(\cos\theta)^N \cos N\theta]. \tag{42}$$

This is a rather unwieldy expression when N is large, but it may be

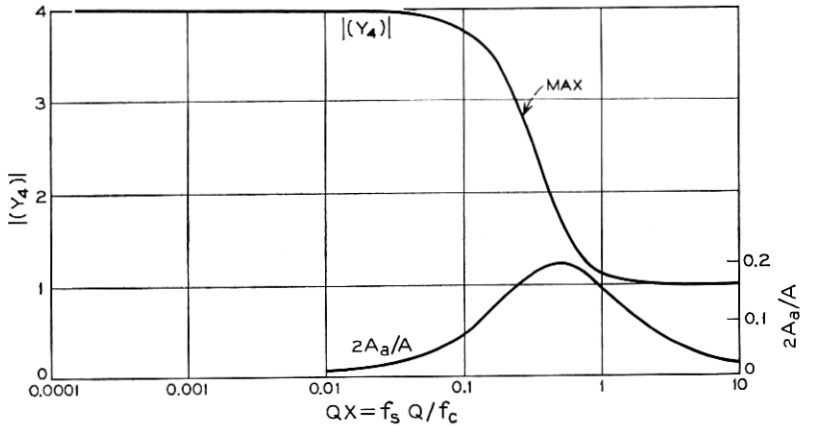

Fig. 11 — Effective transfer characteristic of four tandem timing tank circuits to modulation on pulse train.

approximated for the purpose of finding its maximum value by

$$| \Phi_N | \approx 4K_1 (\cos \theta)^{(1+N/2)} \sin (N\theta/2) \tag{43}$$

since θ is small for large N at the maximum of $| \Phi_N |$. The expression in (43) is maximum with respect to θ when

$$\tan \theta_m \tan (N\theta_m/2) = N/(N + 2). \tag{44}$$

A list of maximum values for Φ_N are given in Table I:

These are plotted in Fig. 14 along with four of the full calculated

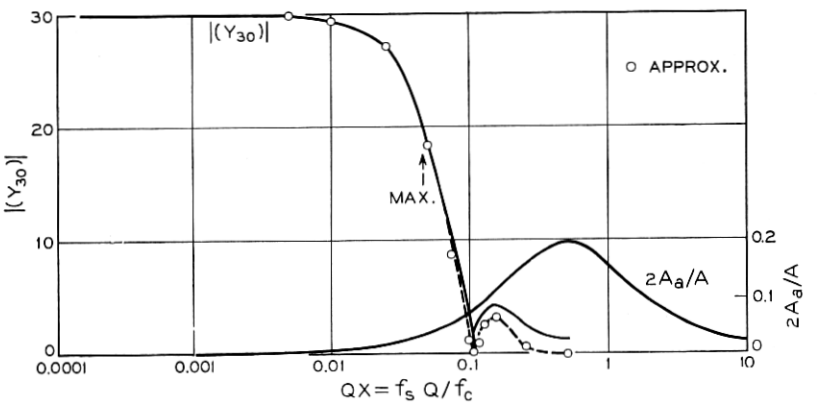

Fig. 12 — Effective transfer characteristic of thirty tandem timing tank circuits to modulation on pulse train.

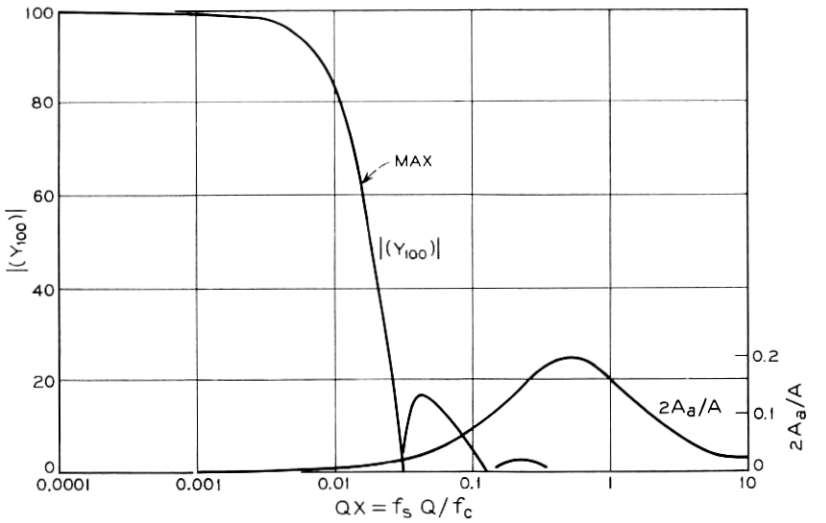

Fig. 13 — Effective transfer characteristic of one hundred tandem timing tank circuits to modulation on pulse train.

spectrum curves of Fig. 2. It is seen from (43) that $4K_1$ is the largest value Φ_N can have.

The spectrum of Φ_1 is plotted along with the $(Y)_N$ function in Figs. 11, 12, and 13 to suggest why the peak values of Φ_N do not increase indefinitely with N.

To get the total mean square "power" of Φ_N, $|\Phi_N|^2$ in (42) is integrated with respect to x from $x = 0$ to ∞ or, with respect to θ, from θ to 0 $-\pi/2$. Since the expression for Φ_N in (42) gives the peak value, we have for the total mean square power P_N,

$$P_N = \frac{1}{2}\int_0^\infty [\Phi_N(\theta)]^2\, df, \tag{45}$$

where a value of 1 Hz is used for the bandwidth B in K_1. Evaluation

TABLE I—MAXIMUM VALUES FOR Φ_m

N	θ_m	Qx_m	Φ_m	
1	$\pi/4$	0.5	K_1	exact
4	0.49	0.267	2.384 K_1	exact
4	0.463	0.249	2.290 K_1	approximate
10	0.2525	0.1290	3.14 K_1	approximate
30	0.0997	0.049	3.68 K_1	approximate
50	0.0603	0.0392	3.80 K_1	approximate
100	0.0308	0.0154	3.90 K_1	approximate

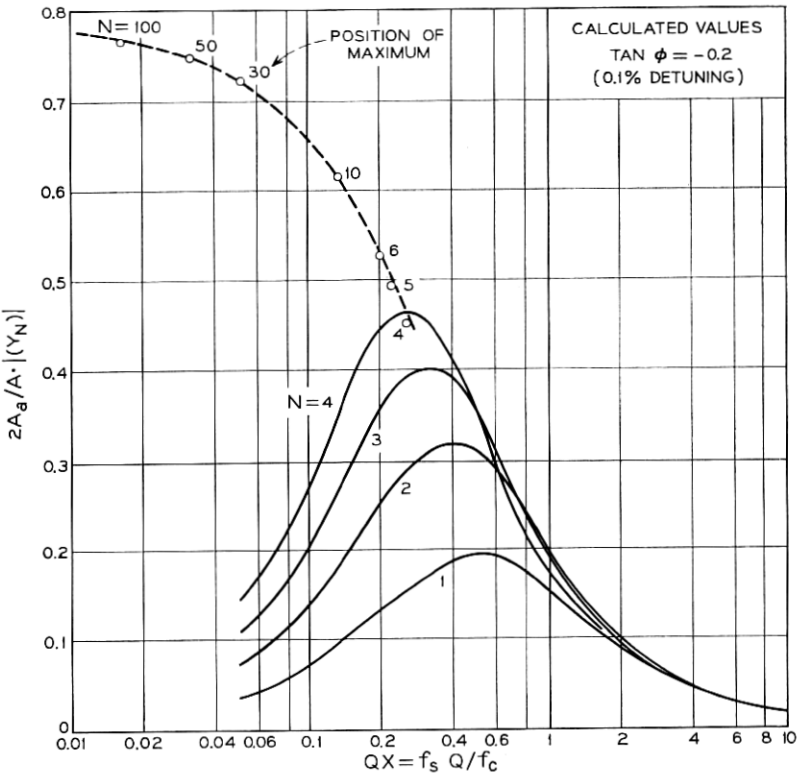

Fig. 14 — Calculated spectra of timing noise caused by tank circuit detuning.

of this integral gives

$$P_N = 2\pi Q \frac{\delta^2}{\omega_c^2}\left\{1 - \frac{1}{2^{N-1}} + \frac{1}{2^{2N}}\frac{(2N)!}{N!\,N!}\right\} \text{ (radians)}^2 \tag{46}$$

ignoring the small difference between ω_o and ω_c . For $N = 1$, we have

$$P_1 = \pi Q\delta^2/\omega_c^2 \tag{47}$$

and for $N \geqq 4$, P_N is approximated very closely by

$$P_N \approx 2\pi Q \frac{\delta^2}{\omega_c^2}\left\{1 - \frac{1}{2^{N-1}} + \frac{1}{(\pi N)^{\frac{1}{2}}}\right\}. \tag{48}$$

Twice the quantity in the braces is plotted in Fig. 15, where exact values from (46) are used through $N = 4$.

The expression in (47) for P_1 was derived in a different way by W. R. Bennett.[1] The expression (46) for P_N has been derived independently and differently by S. O. Rice.

When there is no tank circuit mistuning and amplitude to phase conversion is the only source of phase deviation, that generated at each repeater is given by (27), that is,

$$\Phi_1 = \frac{2(B/f_c)^{\frac{1}{2}} K_L \tan \gamma_o}{[1 + (2qQ/\omega_o)^2]^{\frac{1}{4}}}$$

$$= 2K_o \cos \theta \quad \text{(radians)}. \tag{49}$$

In this case

$$| \Phi_N |^2 = 4K_o^2 \frac{\cos^2 \theta}{\sin^2 \theta} (\cos)^N [(\cos \theta)^N + (\cos \theta)^{-N} - 2 \cos N\theta]. \tag{50}$$

When $(\cos \theta)^N > 0.8$, that is for θ, and hence q, sufficiently small, the sum of the first two terms within the bracket is very close to 2. For this condition, Φ_N may be approximated by

$$| \Phi_N | \approx 4K_o(\cos \theta)^{(1+N/2)} \frac{\sin (N\theta/2)}{\sin \theta}$$

$$\approx 2K_o N[\cos (N\theta/2)](\cos \theta)^{(1+N/2)}, \tag{51}$$

which shows that the phase deviation very near zero frequency increases directly with the number N of repeaters in the chain. This is in contrast with the similar result (43) for mistuning where the largest value of $| \Phi_N |$ is only four times that of $| \Phi_1 |$. $(Y)_N$ is the same for both. The difference arises because of the difference in spectrum shape of the generated phase deviation in the two cases. In mistuning, $| \Phi_1 |$ is zero at zero frequency, while in amplitude to phase conversion effects, $|\Phi_1|$ is flat and nonzero for very low frequencies.

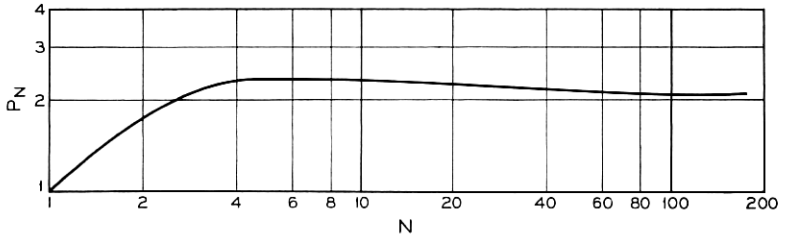

Fig. 15 — Calculated total timing noise caused by tank circuit mistuning as a function of the number N of like repeaters in a chain.

To find the total mean square "power" of Φ_N, the integral (45) is calculated, using (50) this time instead of (42). The value of this integral is given in a paper by Byrne, Karafin, and Robinson.[8] It is

$$P_N = \frac{\pi f_o}{Q} K_o^2 \left\{ N - \frac{1}{2} \frac{(2N-1)!}{4^{(N-1)}[(N-1)!]^2} \right\} \tag{52}$$

which shows that the total phase noise power increases directly with the number N of repeaters in a chain and varies inversely with the Q of the tank circuits.

In Ref. 8, the result (52) and the spectrum (50), or something closely related to it, were derived by assuming that at each repeater there was a noise source (nature and magnitude unknown) with a flat spectrum and "power" density $2K_0^2$. The process followed is similar to work first done by R. C. Chapman of Bell Telephone Laboratories. Also in the paper of Ref. 8, the results of measurements of accumulated timing noise in an experimental $T1$ system are given and the spectra of these are like those of Fig. 3.

2.6 *Spectrum and Phase Noise of Wide Pulses*

In most practical systems it is not desirable for the transmitted pulses arriving at the timing circuit input to have the narrow shape considered in the previous section of the paper. It is to be expected from the above discussions of the effects of dissymmetry between upper and lower side frequencies, that wider pulses having spectra with these characteristics would introduce phase noise in the derived timing wave even when there is no mistuning or amplitude to phase conversion. But the calculation of dissymmetry needs to be more elaborate for the wider pulses; the simple calculation used above is inadequate.

A more generally applicable theory is available from analysis by S. O. Rice who worked it out originally for pulses wide enough to spread over two time slots. How the simple theory is related to the more general one to be described in Section 2.61 will be discussed in Section 2.66. An outline of Rices' analysis follows. It is assumed that neither mistuning nor amplitude to phase conversion is present so that the phase noise calculated is caused by the pulse train alone.

2.6.1 *Fourier Series for Pulse Train*

The general theory is based on a frequency analysis also and so the pulse spectrum is calculated first. We consider the train to consist

of repeated blocks of N pulse periods each, with each of the N pulse periods having a pulse or not at random. The train has a period NT and may be described by the Fourier series

$$I(t) = \sum_{m=-\infty}^{\infty} C_m \exp(j2\pi mt/NT). \tag{53}$$

If the parameter N is made to approach infinity, a random pulse train will be obtained. But a good approximation results if N is just large, say 100.

In order to consider pulses which may be as much as two pulse periods wide so that there is considerable overlapping of adjacent pulses, four auxiliary functions are necessary to specify the current $I(t)$ in any one pulse period of duration T. These functions correspond to the four possibilities of (*i*) no pulse present, (*ii*) only the leading edge of a pulse present, (*iii*) only the trailing edge of a pulse present, and (*iv*) overlapping pulses present.

This is illustrated in Fig. 16 which is a short section in time of a random train of raised cosine pulses exactly two pulse periods wide. The four possibilities mentioned above occur in that order in periods 3, 1, 2, 5 of Fig. 16. For a random train of pulses all these possibilities eventually occur in any one time slot as suggested in the composite drawing of Fig. 17a. In this a number of sections in time of Fig. 16 have been overlapped as they would be in an oscilloscope presentation. In Fig. 17a, the four possibilities in the order given above are *AC, AD, BC, BD*. Another illustration is the same wave after passing through a half-wave rectifier which begins conduction at the half amplitude level as shown in Fig. 17b. Figures 18a and b are photographs of oscilloscope patterns of real pulse trains which approximate the idealized ones of Figs. 17a and b.

Then $I(t)$ may be represented by a sequence of functions $I_n(t)$, each of which is specified by the auxiliary functions $F_2(t')$, $F_3(t')$, $F_4(t')$ and the parameter a_n as follows

$$\begin{aligned} a_n &= 1, \quad a_{n-1} = 1, \quad I_n(t) = F_4(t') \\ a_n &= 1, \quad a_{n-1} = 0, \quad I_n(t) = F_2(t') \\ a_n &= 0, \quad a_{n-1} = 1, \quad I_n(t) = F_3(t') \\ a_n &= 0, \quad a_{n-1} = 0, \quad I_n(t) = 0, \end{aligned} \tag{54}$$

in the time slot interval

$$(n-1)T - \nu T \leqq t \leqq nT - \nu T$$

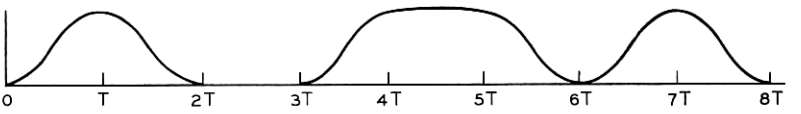

Fig. 16 — Short, time section of a random train of raised cosine pulses, each two time slots wide.

and is zero outside this interval. In this representation, $a_n = 1$ if a pulse begins in the interval under consideration and $a_n = 0$ if a pulse does not begin in it. The time scale t' used for describing the pulse train is related to the time scale t of the Fourier series by

$$t' = t - (n - 1)T + \nu T. \tag{55}$$

The time shift $(n - 1)T$ brings the pulse forms in the nth time slot back to the first one for description by the auxiliary F functions. The

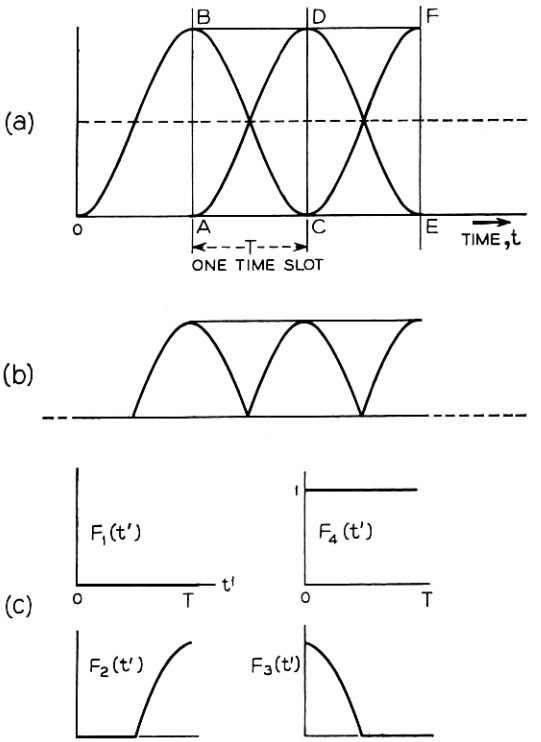

Fig. 17 — Idealized pulse waveforms: (a) Overlapping raised cosine; (b) wave in (a) applied to half-wave rectifier; (c) functions used in calculation.

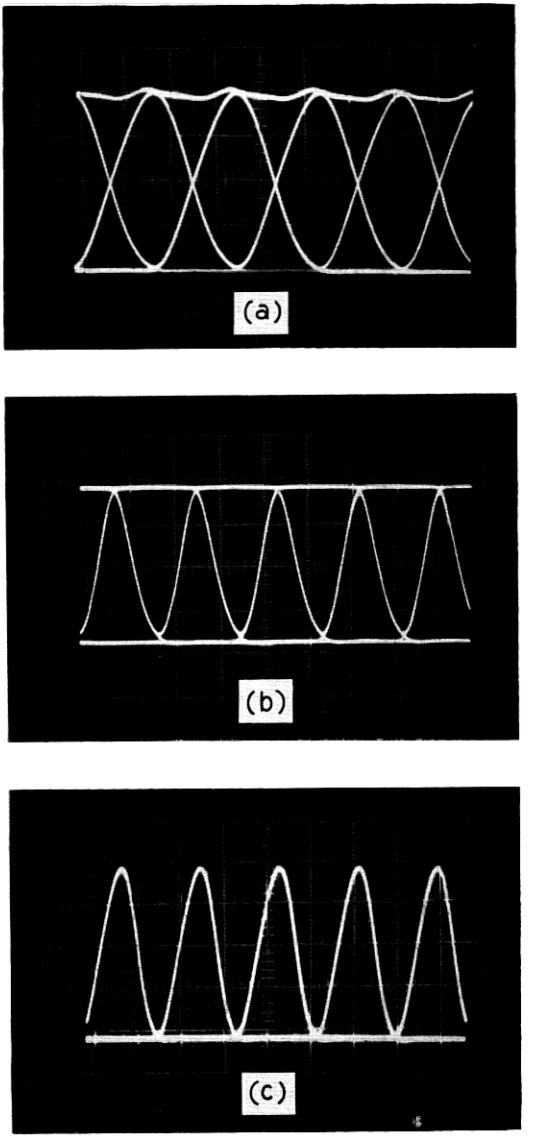

Fig. 18 — Photographs of random pulse oscilloscope traces: (a) Raised cosine pulses, two time slots wide at the base; (b) bottom half of (a) obtained with half-wave rectifier; (c) raised cosine pulses, one time slot wide at the base.

shift νT will be convenient later when it will be desirable to have the occurrence of pulses adjustable with respect to the zeros of the sinusoids in the Fourier series (53). To make $I(t)$ a random pulse train, we let $a_1, a_2, \ldots, a_n \ldots$ be independent random variables with probability of $a_n = 1$ being p and probability of $a_n = 0$ being $q = 1 - p$.

The representation just described was designed with the situation of Fig. 17 in mind; but it is valid for other pulse shapes including those which occupy just one time slot or less. The transformation of time scales is illustrated for rectangular pulses in Fig. 19.

The specifications (54) may be expressed by

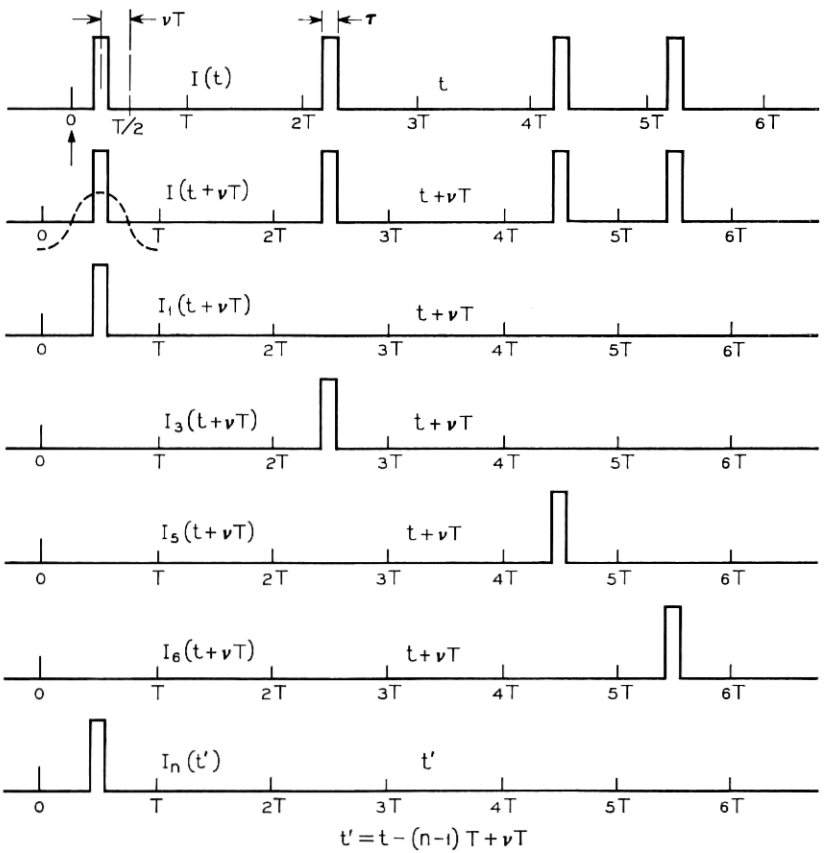

Fig. 19 — Representation of pulse train for Fourier analysis.

$$I_n(t) = a_n(1 - a_{n-1})F_2(t') + a_{n-1}(1 - a_n)F_3(t') + a_n a_{n-1}F_4(t')$$
$$= a_n F_2(t') + a_{n-1}F_3(t') + a_n a_{n-1}[F_4(t') - F_2(t') - F_3(t')] \quad (56)$$

and $I(t)$ is the sum of N separate $I_n(t)$.

2.6.2 *Fourier Coefficients*

The Fourier coefficients C_m in (53) are then

$$C_m = \frac{1}{NT}\int_{-\nu T}^{NT-\nu T} \exp(-j2\pi mt/NT)I(t)\,dt$$
$$= \frac{1}{NT}\sum_{n=1}^{N} \exp[-j2\pi m(n - 1 - \nu)/N]\int_0^T \exp(-j2\pi mt'/NT)$$
$$\cdot I_n[(n - 1 - \nu)T + t']\,dt' \quad (57)$$

where the integral from $-\nu T$ to $NT - \nu T$ has been written in the second form as a sum of N integrals, each over an interval T and then the transformation $t = (n - 1 - \nu)T + t'$ applied to each integral. Let

$$\beta_m = \frac{r_m}{T}\int_0^T \exp(-j2\pi mt'/NT)F_2(t')\,dt' \quad (58)$$

$$\gamma_m = \frac{r_m}{T}\int_0^T \exp(-j2\pi mt'/NT)F_3(t')\,dt' \quad (59)$$

$$\delta_m = \frac{r_m}{T}\int_0^T \exp(-j2\pi mt'/NT)[F_4(t') - F_2(t') - F_3(t')]\,dt \quad (60)$$

$$z = \exp(-j2\pi m/N), \qquad r_m = \exp(j2\pi\nu m/N). \quad (61)$$

Then

$$C_m = \frac{1}{N}\sum_{n=1}^{N} z^{n-1}(a_n\beta_m + a_{n-1}\gamma_m + a_n a_{n-1}\,\delta_m), \quad (62)$$

and the average value of C_m is

$$\langle C_m\rangle_{\text{av}} = \frac{1}{N}\sum_{n=1}^{N} z^{n-1}(p\beta_m + p\gamma_m + p^2\,\delta_m). \quad (63)$$

Since

$$\sum_{n=1}^{N} z^{n-1} = 0 \qquad m \neq lN$$
$$= N \qquad m = lN,$$

where l is an integer, we have

$$\langle C_m\rangle_{\text{av}} = p(\beta_m + \gamma_m + p\ \delta_m), \qquad m = 0, \quad \pm N, \quad \pm 2N, \cdots,$$
$$\langle C_m\rangle_{\text{av}} = 0, \qquad \text{otherwise.} \tag{64}$$

The Fourier components for $m = \pm N$ are those at the fundamental frequency of the pulse rate, $1/T$. The average values of the "noise" components are all zero but the second order averages are not zero. Rices' calculation of these follows.

From the expressions for C_m and $\langle C_m\rangle_{\text{av}}$ in (62) and (63), it follows that

$$\begin{aligned}(C_m - \langle C_m\rangle_{\text{av}})(C_l - \langle C_l\rangle_{\text{av}}) \\ = N^{-2} \sum_{n=1}^{N}\sum_{k=1}^{N} z^{n-1}\zeta^{k-1}[(a_n - p)\beta_m + (a_{n-1} - p)\gamma_m + (a_n a_{n-1} - p^2)\ \delta_m] \\ \cdot[(a_k - p)\beta_l + (a_{k-1} - p)\gamma_l + (a_k a_{k-1} - p^2)\ \delta_l]\end{aligned} \tag{65}$$

where $\zeta = \exp(-j2\pi l/N)$. Expanding the last product and using the independence of the a_n's (except for $a_o = a_N$) shows that the ensemble average of (65) depends upon the averages

$$\begin{aligned}\langle (a_n - p)^2\rangle_{\text{av}} &= p - p^2 = pq \\ \langle (a_n - p)(a_n a_j - p^2)\rangle_{\text{av}} &= p^2 - p^3 = p^2 q, \qquad j \neq n \\ \langle (a_n a_{n-1} - p^2)^2\rangle_{\text{av}} &= p^2 - p^4 \\ \langle (a_n a_j - p^2)(a_n a_i - p^2)\rangle_{\text{av}} &= p^3 - p^4 = p^3 q, \\ & \qquad j \neq n, \qquad i \neq n, \qquad i \neq j.\end{aligned} \tag{66}$$

For n fixed, the only values of k which lead to nonzero averages are $k = n$ and $k = n \pm 1$ with the understanding that for $n = 1$ the values $k = 0, 1, 2$ mean $k = N, 1, 2$, and for $n = N$ the values $k = N - 1, N, N + 1$ mean $k = N - 1, N, 1$. When $k = n$ the average value of the summand in (65) is

$$\begin{aligned}z^{n-1}\zeta^{n-1}[pq\beta_m\beta_l + pq\gamma_m\gamma_l + (p^2 - p^4)\ \delta_m\ \delta_l \\ + p^2 q(\beta_m\ \delta_l + \gamma_m\ \delta_l + \delta_m\beta_l + \delta_m\gamma_l)].\end{aligned} \tag{67}$$

For $k = n + 1$ it is

$$z^{n-1}\zeta^{n}[pq\beta_m\gamma_l + p^2 q(\beta_m\delta_l + \delta_m\gamma_l) + p^3 q\delta_m\delta_l], \tag{68}$$

and for $k = n - 1$,

$$z^{n-1}\zeta^{n-2}[pq\gamma_m\beta_l + p^2 q(\gamma_{ml} + \delta_m\beta_l) + p^3 q\delta_m\delta_l]. \tag{69}$$

Some experimentation shows that the sum of (67), (68), and (69) can be written as

$$(z\zeta)^{n-1}[pq\{\beta_m y + \gamma_m y^{-1} + p\delta_m(y + y^{-1})\} \cdot \{\beta_l y^{-1} + \gamma_l y + p\delta_l(y^{-1} + y)\} + p^2q^2\delta_m\delta_l], \tag{70}$$

where

$$y = \zeta^{\frac{1}{2}} = \exp(-j\pi l/N). \tag{71}$$

The sum of $(z\zeta)^{n-1}$, taken from $n = 1$ to N, is 0 unless $z\zeta = 1$, that is, unless $M + l = 0, \pm N, \pm 2N, \ldots$. In this case

$$N^{-2}\sum_{n=1}^{N}(z\zeta)^{n-1} = N^{-1}, \qquad \zeta = z^{-1} = \exp(+j2\pi m/N),$$

$$y = \exp(-j\pi l/N) = \exp[-j\pi(l + m)/N]\exp(+j\pi m/N)$$

$$= (-1)^{(l+m)/N}\exp(j\pi m/N), \tag{72}$$

and (70) can be written as

$$[pq(-1)^{(l+m)/N}S_mS_l + p^2q^2\delta_m\delta_l] \tag{73}$$

where

$$S_m = \beta_m\exp(j\pi m/N) + \gamma_m\exp(-j\pi m/N) + 2p\,\delta_m\cos\frac{\pi m}{N}, \tag{74}$$

and S_l is defined similarly with l in place of m, and δ_m is the function defined in (60).

Collecting results shows that averaging (65) over the ensemble gives

$$\langle(C_m - \langle C_m\rangle_{av})(C_l - \langle C_l\rangle_{av})\rangle = \begin{cases} [pq(-1)^{(m+l)/N}S_mS_l + p^2q^2\,\delta_m\,\delta_l]/N, \\ \qquad m + l = 0, \quad \pm N, \quad \pm 2N, \cdots \\ 0, \quad \text{otherwise} \end{cases} \tag{75}$$

Replacing $C_l - \langle C_l\rangle_{av}$, ζ, β_l, γ_l, δ_l, y by their complex conjugates in expressions (65) to (71), and noting that the sum of $(z\zeta^*)^{n-1}$ is zero unless $z\zeta^* = 1$, that is, unless $m - l = 0, \pm N, \pm 2N, \cdots$, carries (75) into

$$\langle (C_m - \langle C_m \rangle_{av})(C_l - \langle C_l \rangle_{av})^* \rangle = \begin{cases} [pq(-1)^{(m-l)/N} S_m S_l^* + p^2 q^2 \, \delta_m \, \delta_l^*]/N, \\ \qquad m - l = 0, \quad \pm N, \quad \pm 2N, \cdots . \\ 0, \quad \text{otherwise} \end{cases} \tag{76}$$

In terms of the functions $F_j(t)$ we have

$$\delta_m = \frac{\tau_m}{T} \int_0^T \exp(-j2\pi mt/NT)[F_4 - F_3 - F_2] \, dt$$

$$S_m = \frac{\tau_m}{T} \int_0^T \exp(-j2\pi mt/NT) \left\{ [2pF_4 + (q-p)F_3 + (q-p)F_2] \cdot \cos \frac{\pi m}{N} + j[F_2 - F_3] \sin \frac{\pi m}{N} \right\} dt. \tag{77}$$

The mean square value of the noise component of frequency m/NT is

$$\sigma_m^2 = 4\langle C_m C_m^* \rangle_{av} , \tag{78}$$

considering a positive frequency only spectrum. Thus from (76), we get

$$\sigma_m^2 = 4pq[S_m S_m^* + pq \, \delta_m \, \delta_m^*] \frac{1}{N}. \tag{79}$$

2.6.3 *Phase Modulation of Tuned Circuit Response*

To calculate the phase modulation on the recovered fundamental, we first obtain the response of the tank circuit to the train of rectified pulses, $I(t)$. This response is the approximate sine wave at the pulse rate frequency.

The response $I_o(t)$ is described by

$$I_o(t) = R_o(t) \cos [2\pi f_c t + \varphi(t)] \tag{80}$$

where the envelope $R_o(t)$ and the phase angle $\varphi(t)$ are slowly fluctuating functions whose rate of change is proportional to the bandwidth of the tank circuit. Considering now, only those components of $I(t)$ in the vicinity of the pulse rate $1/T$, we have

$$I_o(t) = 2\text{Re} \sum_{m \approx N} Y_m C_m \exp(j2\pi mt/NT). \tag{81}$$

Writing $C_m = (C_m - \langle C_m \rangle_{av}) + \langle C_m \rangle_{av}$ and noting that $\langle C_N \rangle_{av}$ is the only nonzero value of $\langle C_m \rangle_{av}$ in the summation, (81) may be rearranged* to be

* Y_N as used here is Y_m for $m = N$ and is not the $(Y)_N$ of Section 2.5.

$$I_o(t) = 2\mathrm{Re}\{Y_N\langle C_N\rangle_{av} \exp(j2\pi t/T) + \sum_{m\approx N} Y_m(C_m - \langle C_m\rangle_{av}) \exp(j2\pi mt/T)\}$$

$$= 2\mathrm{Re}\, Y_N\langle C_N\rangle_{av} \exp(j2\pi t/T) \cdot\left\{1 + \sum_{m\approx N} \frac{Y_m(C_m - \langle C_m\rangle_{av}) \exp[j2\pi(m - N)t/NT]}{Y_N\langle C_N\rangle_{av}}\right\}. \quad (82)$$

The summation part of this is small, partly because σ_m/σ_N is small and partly because of the attenuation of the tank circuit Y_m except for frequencies near the pulse rate $1/T$. Thus if the part within the brackets is represented by $1 + A + jB$, $|A + jB|$ is small compared with unity and so

$$1 + A + jB \approx \exp[A + jB] \quad (83)$$

and

$$I_o(t) \approx 2\mathrm{Re}\, Y_N\langle C_N\rangle_{av} \exp[j(2\pi t/T) + A + jB]$$

$$\approx 2\,|\,Y_N\langle C_N\rangle_{av} \exp(A)\,|\cos[2\pi t/T) + B + \arg(Y_N\langle C_N\rangle_{av})]. \quad (84)$$

This is the approximate sine wave at the pulse rate frequency which has been recovered from the pulse train by means of the narrowband tank circuit. Its phase modulation is

$$\varphi(t) = \arg(Y_N\langle C_N\rangle_{av}) + B$$

$$= \arg(Y_N\langle C_N\rangle_{av}) + \mathrm{Im} \sum_{m\approx N} b_m \exp[j2\pi(m - N)t/NT] \quad (85)$$

where

$$b_m = Y_m(C_m - \langle C_m\rangle_{av})/(Y_N\langle C_N\rangle_{av}). \quad (86)$$

The Fourier component of $\varphi(t)$ at frequency k/NT is determined by the two side frequencies $mf_c/N = (N + k)/NT$ and $mf_c/N = (N - k)/NT$ about the pulse rate as was found in the earlier analysis. To calculate this, we use the two terms for which $m = N \pm k$ in the above sum. That is

$$\varphi_k = \mathrm{Im}[b_{N+k} \exp(j2\pi kt/NT) + b_{N-k} \exp(-j2\pi kt/NT)]$$

$$= \mathrm{Im}[(b_{N+k} - b^*_{N-k}) \exp(j2\pi kt/NT)]. \quad (87)$$

The time average of the "phase power" in this component is

$$\langle\varphi_k^2\rangle_{avt} = \tfrac{1}{2}\,|\,b_{N+k} - b^*_{N-k}\,|^2 \text{ radians}^2 \quad (88)$$

which can be written

$$\langle \varphi_k^2 \rangle_{av\,t} = \tfrac{1}{2}[b_+ b_+^* - b_+ b_- - b_-^* b_+^* + b_-^* b_-] \tag{89}$$

where the subscripts + and − denote $N \pm k$.

The ensemble average of the expression (89) may be computed with the help of the second order moments of the C_m's given by (75) and (76). For example

$$\begin{aligned} \langle b_+ b_+^* \rangle_{av} &= Y_+ Y_+^* \langle (C_{N+k} - \langle C_{N+k} \rangle_{av})(C_{N+k} - \langle C_{N+k} \rangle_{av})^* \rangle / |\, Y_N \langle C_N \rangle_{av} |^2 \\ &= Y_+ Y_+^* (pqS_+ S_+^* + p^2 q^2\, \delta_+\, \delta_+^*) / |\, Y_N \langle C_N \rangle_{av} \,|^2\, N \\ &= [pqU_+ U_+^* + p^2 q^2 V_+ V_+^*]/N \end{aligned} \tag{90}$$

where

$$U_+ = (Y_+/Y_N)(S_+/\langle C_N \rangle_{av}) \quad V_+ = (Y_+/Y_N)(\delta_+/\langle C_N \rangle_{av}) \tag{91}$$

and the subscripts + and − are used to indicate $m_\pm = N \pm k$. Also $m - l = (N + k) - (N + k) = 0$ so that the (-1) to the power $(m - l)/N$ appearing in (26) is $+1$. Similarly, in the calculation of $\langle b_+ b_- \rangle$, $m + l = (N + k) + (N - k) = 2N$ and the (-1) to the power $(m + l)/N$ appearing in (75) is again $+1$, and so on.

After the ensemble average of (90) has been calculated, taking each of the four parts of (90) in turn, the terms may be combined to give one of the results we have been seeking:

$$\langle \varphi_k^2 \rangle_{av} = \frac{1}{2} \frac{pq}{N} \{ |\, U_+ - U_-^* \,|^2 + pq \,|\, V_+ - V_-^* \,|^2 \} \quad \text{radians}^2. \tag{92}$$

Since the Fourier components are f_c/N apart, this expression for φ_k^2 is equivalent to the "phase power" in a band f_c/N wide. The averaging has been done over both time and the ensemble.

2.6.4. *Effect of Sampling and of High Frequencies in the Response*

Next we consider a generalization of the expression (92) as derived above for the phase modulation on the fundamental pulse rate obtained by passing the random pulse train through a tuned circuit.

In deriving the result (92) for the phase modulation of the timing wave obtained from the tuned circuit response, only that part of the pulse train spectrum in the vicinity of the pulse rate was considered.

While the major part of the tuned circuit response lies in the frequency region near the pulse rate $1/T$, as assumed in the calculation beginning with (81) and ending with (92), the way in which this

response is used in a regenerative repeater (or is measured in a phase detector) gives some importance to the part of the response neglected in (81).

In a regenerative repeater, retiming of the message pulses is done by very sharp pulses which are generated at each positive (or negative) going zero crossing of the timing wave. In the phase detector used in the experiments described here, the deviations of the zero crossings from their ideal periodic nature are measured and used as a sequence of numbers or held and smoothed by low pass filter to approximate the phase deviation function $\varphi(t)$. Thus in both these processes, it is the samples of the derived timing wave which are used. When the deviations are not too large, the magnitudes of the zero crossing deviations are equivalent to the magnitudes of samples of the phase deviation wave $\varphi(t)$, taken at the pulse rate. Since the high frequency part of the tuned circuit response which was neglected in (81) lies above one-half the sampling rate, the process described above as equivalent to sampling, may convert some of this high frequency part into very low frequency energy in the final timing noise result. In particular, if the high frequency part of the pulse spectrum has energy at or very near the harmonics of the pulse rate, this will be converted to zero or very low frequency energy in the phase noise spectrum. The analysis by S. O. Rice deals with this situation also.

First the expression (81) for $I_o(t)$ must be enlarged to include a dc term and all values of m from 1 to ∞. This may be rewritten in the following form which corresponds to (83). We have

$$I_o(t) = 2 \operatorname{Re} Y_N C_N \exp(j2\pi t/T)\Big\{1 + \tfrac{1}{2} d_o \exp(-j2\pi t/T) + \sum_{l=2}^{\infty} d_l \exp[j2\pi(l-1)t/T] + \tfrac{1}{2} b_o \exp(-j2\pi t/T) + \sum_{m=1}^{\infty} b_m \exp[j2\pi(m-N)t/NT]\Big\} \tag{93}$$

where l is an integer,

$$d_l = Y_{Nl}\langle C_{Nl}\rangle_{av}/Y_N\langle C_N\rangle_{av}$$

and the coefficient b_m is defined as in (86). This expression is the complete response of the tuned circuit to the random train of pulses.

Again assuming that the term within the square brackets in (93)

always remains near 1,

$$\varphi(t) \approx \arg Y_N\langle C_N\rangle_{av} + \text{Im}\left\{\tfrac{1}{2}d_o \exp(-j2\pi t/T) + \sum_{l=2}^{\infty} d_l \exp[j2\pi(l-1)t/T]\right\} + \text{Im}\left\{\tfrac{1}{2}b_o \exp(-j2\pi t/T) + \sum_{m=1}^{\infty} b_m \exp[j2\pi(m-N)t/NT]\right\}. \quad (94)$$

This is an improved version of (85). The first line on the right is approximately the ensemble average $\langle\varphi(t)\rangle_{av}$. It consists of a dc term and harmonics of the pulse repetition frequency $1/T$. While it may appear that the assumption about the bracketed part of (94) being small is unjustified because this represents the adding of harmonics to yield the pulse wave form, this is not the case since all the harmonics included are reduced at least by Q. Furthermore, since the sampling operation occurs near the zeros of the response, where the harmonics are zero or very small, an additional reduction of magnitude is involved. The noise portion of the power spectrum of $\varphi(t)$ arises from the second line, which may be written as

$$\varphi(t) - \langle\varphi(t)\rangle_{av} \approx \text{Im}\left[\tfrac{1}{2}b_o \exp(-j2\pi t/T) + \sum_{k=1-N}^{\infty} b_{N+k} \exp(j2\pi kt/TN)\right]. \quad (95)$$

The sampling operation mentioned above, which is performed on the phase function $\varphi(t)$ in both the phase detector used in the experiments reported and in regenerative PCM repeaters, generates a new phase function $\theta(t)$. This is

$$\theta(t) \approx \varphi(t)T \sum_{n=-\infty}^{\infty} \hat{\delta}(t - nT) = \varphi(t) \sum_{n=-\infty}^{\infty} \exp(j2\pi nt/T) \quad (96)$$

where $\hat{\delta}(t)$ denotes the unit impulse function. For some frequencies in $\varphi(t)$, the extraneous modulation products introduced by the impulses may be negligible. However, for the higher frequencies and for a single tuned circuit with slowly decreasing $Y(i\omega)$, some of the products may become appreciable and should be taken into account. The sampling times in (96) were arbitrarily set at $t = 0, T, 2T \cdots$ for convenience in the analysis to follow. These can be varied to occur at or near the zeros of the response wave $I_o(t)$ by shifting the time scale of the description of the pulse train using the parameter ν as indicated by (54) and related equations as illustrated in Fig. 19. Forming the ensemble average

$\langle\theta(t)\rangle_{av}$, subtracting it from $\theta(t)$, and noticing that the sums in the expression (96) for $\theta(t)$ are real, leads to

$$\theta(t) - \langle\theta(t)\rangle_{av} = \operatorname{Im}\left\{\tfrac{1}{2}b_o \sum_{n=-\infty}^{\infty} \exp(j2\pi nt/T) + \sum_{n=-\infty}^{\infty}\sum_{k=1-N}^{\infty} b_{N+k} \exp[j2\pi(k+nN)t/NT]\right\}. \quad (97)$$

The component of $\theta(t)$ of frequency l/NT for $1 \leqq l \leqq N-1$, that is, for frequencies which lie between 0 and f_o, is the sum of terms having exponential factors $\exp(\pm j2\pi lt/NT)$. For $k + nN = +l$, the values of k and n are

$$k = -N + l, \quad k = l, \quad k = N + l, \quad k = 2N + l, \cdots,$$
$$n = 1, \quad n = 0, \quad n = -1, \quad n = -2, \cdots,$$

and for $k + nN = -l$ they are

$$k = -l, \quad k = N - l, \quad k = 2N - l, \cdots,$$
$$n = 0, \quad n = -1, \quad n = -2, \cdots,$$

Therefore the component of $\theta(t)$ of frequency l/NT is

$$\begin{aligned}&\operatorname{Im}[(b_l + b_{N+l} + b_{2N+l} + \cdots)\exp(j2\pi lt/NT) \\ &\quad + (b_{N-l} + b_{2N-l} + b_{3N-l} + \cdots)\exp(-j2\pi l/NT] \\ &= \operatorname{Im}[\{(b_l + b_{N+l} + b_{2N+l} + \cdots) - (b_{N-l} + b_{2N-l} + \cdots)^*\} \\ &\quad \cdot \exp(j2\pi lt/NT).\end{aligned} \quad (98)$$

When b_{N+l} and b_{N-l} are the dominant terms in (98), comparison with expression (87) (with $k = l$) shows that the component of $\theta(t)$ of frequency l/NT is nearly equal to the corresponding component in $\varphi(t)$. By means of the procedure used earlier in (91) the average power in the component of $\theta(t)$ of frequency k/NT is obtained where we have returned to k from the l in (98). First, the time average of the power in the component is

$$\begin{aligned}\langle\theta_k^2\rangle_{av\,t} &= \frac{1}{2}\left|\sum_{n=0}^{\infty} b_{nN+k} - \sum_{n=1}^{\infty} b_{nN-k}^*\right|^2 \\ &= \frac{1}{2}\left[\sum_{n=0}^{\infty} b_{nN+k} - \sum_{n=1}^{\infty} b_{nN-k}^*\right]\left[\sum_{n=0}^{\infty} b_{nN+k}^* - \sum_{n=1}^{\infty} b_{nN-k}\right]\end{aligned} \quad (99)$$

where $0 < k < n$. To average (99) over the ensemble we make use

of (75) and (76) slightly rewritten by substituting $\exp(-j\pi m/N)$ for $(-1)^{m/N}$ and including it with S_m. Thus

$$\langle (C_m - \langle C_m \rangle_{av})(C_l - \langle C_l \rangle_{av}) \rangle$$

$$= \frac{pq}{N} [S_m \exp(-j\pi m/N)][S_l \exp(-j\pi l/N)] + \frac{p^2q^2}{N} \delta_m \delta_l ,$$

$$m + l = 0, \pm N, \pm 2N, \cdots , \tag{100}$$

$$\langle (C_m - \langle C_m \rangle_{av})(C_l - \langle C_l \rangle_{av})^* \rangle_{av}$$

$$= \frac{pq}{N} [S_m \exp(-j\pi m/N)][S_l \exp(-j\pi l/N)]^* + \frac{p^2q^2}{N} \delta_m \delta_l^*$$

$$m - l = 0, \pm N, \pm 2N, \cdots . \tag{101}$$

The averages are equal to zero unless m and l satisfy the respective conditions.

A typical term encountered in the averaging of (99) is

$$\langle b_{nN+k} b^*_{n'N+k} \rangle_{av} = \langle b_m b^*_l \rangle_{av}$$

where $m = nN + k$, $l = n'N + k$, and $m - l = (n - n')N$. From (101)

$$\langle b_m b^*_l \rangle_{av} = \frac{pq}{N} [U_m \exp(-j\pi m/N)][U_l \exp(-j\pi l/N)]^* + \frac{p^2q^2}{N} V_m V_l^* ,$$

$$m - l = (n - n')N.$$

In this U and V are generalized from the definitions of (91), so that for example

$$U_{nN+k} = \frac{S_{nN+k}}{\langle C_N \rangle_{av}} \frac{Y_{nN+k}}{Y_N}. \tag{102}$$

Considering all four forms of $\langle b_m b \rangle_{av}$ as before, the ensemble average of (99) is found to be

$$\langle \theta_k^2 \rangle_{av} = \frac{pq}{2N} \left| \sum_{n=0}^{\infty} U_{nN+k} \exp[-j\pi(nN + k)/N] - \sum_{n=1}^{\infty} U^*_{nN-k} \exp[+j\pi(nN - k)/N] \right|^2$$

$$+ \frac{p^2q^2}{2N} \left| \sum_{n=0}^{\infty} V_{nN+k} - \sum_{n=1}^{\infty} V^*_{nN-k} \right|^2 \text{(radians)}^2. \tag{103}$$

The $\exp(-j\pi k/N)$ can be factored from the first absolute value and

then exp $(\pm j\pi nN/N)$ replaced by $(-1)^n$, so that

$$\langle\theta_k^2\rangle_{av} = \frac{pq}{2N}\left|\sum_{n=0}^{\infty}(-)^n U_{nN+k} - \sum_{n=1}^{\infty}(-)^n U^*_{nN-k}\right|^2 + \frac{p^2q^2}{2N}\left|\sum_{n=0}^{\infty} V_{nN+k} - \sum_{n=1}^{\infty} V^*_{nN-k}\right|^2 \text{(radians)}^2, \quad (104)$$

which is the generalization of (92) when the complete response of the tuned circuit is used. To repeat what was said before, since the Fourier components in the spectrum of θ are f_c/N apart, this expression for $\langle\theta_k^2\rangle_{av}$ at $f = k/NT$ is equivalent to the "phase power" in a band f_c/N wide in a continuous spectrum.

To obtain the continuous power spectrum $w_\theta(f)$ of the "noise" part of θ, we let $m/NT = f'$ and $N \to \infty$ in the above expressions. First (77) becomes

$$\delta(f') = \frac{\exp(j2\pi\nu f'/f_c)}{T}\int_0^T \exp(-j2\pi f' t)[F_4 - F_3 - F_2]\,dt$$

$$S(f') = \frac{\exp(j2\pi\nu f'/f_c)}{T}\int_0^T \exp(-j2\pi f' t)\{[2pF_4 + (q-p)F_3 + (q-p)F_2]\cos\pi f'T + j[F_2 - F_3]\sin\pi f'T\}\,dt. \quad (105)$$

Also

$$U_{nN+k} \to U(f') = U(nf_c + f) = \frac{Y[j2\pi(nf_c+f)]}{Y(j2\pi f_c)}\,\frac{S(nf_c+f)}{p[S(f_c) + p\,\delta(f_c)]} \quad (106)$$

where $\langle C_N\rangle_{av}$ has been replaced by $p(S_N + p\delta_N)$ as derived from (64) and (74).

Since the expressions derived earlier for the average power in a component of $\varphi(t)$ refer to positive frequency only, we shall deal with the one-sided power spectrum $w_\theta(f)$ of $\theta(t)$. As before $f = k/NT$ denotes the frequency associated with the average power expressed in (104). Then the value of the right side of (104) tends to $w(f)\Delta f = w_\theta(f)/NT$ as $N \to \infty$ and consequently

$$w_\theta(f) \approx \frac{Tpq}{2}\left|\sum_{n=0}^{\infty}(-)^n U(nf_c + f) - \sum_{n=1}^{\infty}(-)^n U^*(nf_c - f)\right|^2 + \frac{Tp^2q^2}{2}\left|\sum_{n=0}^{\infty} V(nf_c + f) - \sum_{n=1}^{\infty} V^*(nf_c - f)\right|^2 \text{(radians)}^2 \text{ per Hz}, \quad (107)$$

where $0 < f < f_c$.

2.6.5 *Application of Results in Section 2.6.4 to Particular Pulse Shapes*

Comparing the result (104) with the earlier (92), it is seen that each component of frequency $f = k/NT$ in the spectrum of θ is made up of contributions from the pairs of components spaced f from all the harmonics of the pulse rate f_c. The sampling of $\phi(t)$ has brought in all these additional contributions.

Now we are in a position to find out what the effect is of neglecting the higher frequencies as was done in the previous work and especially in deriving the result (92) to which (104) reduces when only $n = 1$ is considered.

To do this, we will investigate several particular pulse shapes. As will be seen below, certain simplifications arise for $n = 1$ so that in some cases, approximate expressions for the noise may be derived. But, in general, and especially when the sums of (107) are to be calculated, the expressions become so complex that they cannot be dealt with readily in an analytical way. However, numerical calculations of $w_\theta(f)$ in (107) answers most of our questions. Some of the computations for the rectangular pulses were first done by S. O. Rice. The others are extensions of them. The sums were carried to 30 terms for the rectangular pulses and to 15 or 20 in the other cases. Leveling off occurred before these cutoff points were reached.

If each pulse is confined to one time slot, then $I_n(t)$ is determined entirely by a_n. Thus, in the specifications (54), we have

$$F_3(t') = 0; \qquad F_2(t') = F_4(t'). \tag{108}$$

As a consequence, it is seen from (59), (60), and (74) that

$$\delta_m = 0, \qquad \gamma_m = 0 \tag{109}$$

$$S_m = \beta_m \exp(j\pi m/N) \tag{110}$$

with corresponding simplifications in (75), (76), (79), and (92) and (104).

2.6.5.1 *Narrow Rectangular Pulse.* First take the rectangular pulse of duration τ used in Fig. 19. Here

$$\begin{aligned} F_2(t') = F_4(t') &= 1, \qquad (T - \tau)/2 < t' < (T + \tau)/2 \\ &= 0, \qquad \text{elsewhere.} \end{aligned} \tag{111}$$

Calculation of the pulse spectrum function S_m from (110), (58), and (61) yields

$$\frac{S_m}{S_N} = (-)^{n-1} \exp\,[j\pi x(1 - 2\nu)] \frac{\exp\,[-j\pi 2\nu(n-1)]}{(n+x)} \frac{\sin \pi(n+x)\tau/T}{\sin \pi\tau/T} \tag{112}$$

using $m = nN + k$ and $x = k/N$.

The expression (3) in Section 2.1 for the ratio of noise power in a band B to carrier power is derived from (112) using (79) and (64), putting f'/f_c for $n + x$, and noting that $\sigma_N = 2pS_N$ for a positive frequency only spectrum as in (79). Thus

$$\begin{aligned} \frac{\sigma_m^2}{\sigma_N^2} &= \frac{q}{pN} \frac{S_m S_m^*}{S_N^2} \\ &= \frac{f_c^2}{N} \frac{\sin^2 \pi f'\tau}{(f')^2 \sin^2 \pi\tau/T}. \end{aligned} \tag{113}$$

These components are f_c/N apart and so the power of each corresponds to that in a band B of this width. The ratio σ_m^2/σ_N^2 corresponds exactly to S^2/A_i^2 in (3).

To apply these results to the single tuned tank circuit centered on the pulse rate, the general form of Y_{m+}/Y_N as given in (15) is necessary. This is

$$Y_{nN+k}/Y_N = \frac{n+x}{n + x + jQ[(n+x)^2 - 1]}. \tag{15}$$

Combining (15) with (112) in (102) or (106) gives

$$\begin{aligned} &U(nf_c + f) \\ &= \frac{(-)^{n-1} \exp\,[j\pi x(1-2\nu)] \exp\,[-j\pi 2\nu(n-1)]}{p[n + x + jQ[(n+x)^2 - 1]]} \frac{\sin \pi(n+x)\tau/T}{\sin \pi\tau/T} \end{aligned} \tag{114}$$

with $f' = nf_c + f$ and $m/N = f'/f_c$.

First, notice that the factor $\exp\,(j2\pi x\nu)$ in (114) disappears in the calculation of (107) since $\exp\,(j\pi x2\nu) = \exp^*\,(j\pi(-x)2\nu)$ and hence factors out of both sums.

Next consider the unique conditions that arise when $n = 1$. The second exponential factor containing the parameter ν, which determines the sampling time, disappears from (114). And the factor multiplying jQ in the denominator becomes proportional to x. The first means that the sampling time has no effect on the contribution of the $n = 1$ terms to $w_\theta(f)$. The second means that $(U_+ - U_-^*) \to 0$ as $x \to 0$ and hence that the contribution of $n = 1$ to $w_\theta(f)$ approaches zero as $f \to 0$.

As indicated in Fig. 19, the zero crossing of the fundamental component comes at the $t = 0$ sampling time for $\nu = \frac{1}{4}$; hence this value was used in the computations. Timing noise spectra obtained in this way for several durations of rectangular pulse are plotted in Fig. 20. In order that the effect of the high frequencies may be easily seen, the corresponding spectra considering only the $n = 1$ term are shown in Fig. 21.

Several interesting points are evident:

(*i*) Comparing the two sets of spectra, it is seen that the high frequencies have brought in noise at and near zero frequency, except for the $\tau/T = 0.6$ duration.*

(*ii*) There is a great difference in the full spectra for $\tau/T > 0.5$. This was observed experimentally for other values of τ/T than 0.6.

(*iii*) The high frequencies in the timing tank response, through the sampling process, have not only brought in very low frequency phase noise, but reduced the higher frequency noise except for $\tau/T = 0.6$. It is the phase structure of this noise which makes cancellation as well as addition possible.

(*iv*) In the case of $\tau/T = 0.6$, there is only a small difference between the spectrum obtained with the full spectrum and that from considering only $n = 1$.

(*v*) There is very little difference between the spectra for $\tau/T = 0.1$ and $\tau/T = 0.02$. This suggests that the phase noise may not disappear for pulses which approach spikes in shape.

(*vi*) The magnitude of the noise, when compared with that of the usually more practical rounded shapes, is quite small, as seen in Fig. 4. It will be seen below, that the effect of the high frequencies is much less for these other pulse shapes.

For the narrow pulse case, $\tau/T = 0.1$, the timing noise spectrum can be changed greatly by small amounts of tank circuit mistuning, as shown in Fig. 22. This also can be a cancellation or an addition effect.

When the tank circuit is mistuned from the pulse rate, $\pm x$ is replaced by $x_o \pm x$ in (15) for the normalized admittance. Here x_o is the relative mistuning as defined earlier in (18).

2.6.5.2 *1T Raised Cosine Pulse.* A photograph of an oscilloscope display of this pulse shape is given in Fig. 18c. Each pulse is confined to

---

* The possibility of this property of the noise was pointed out by H. E. Rowe. See Ref. 6.

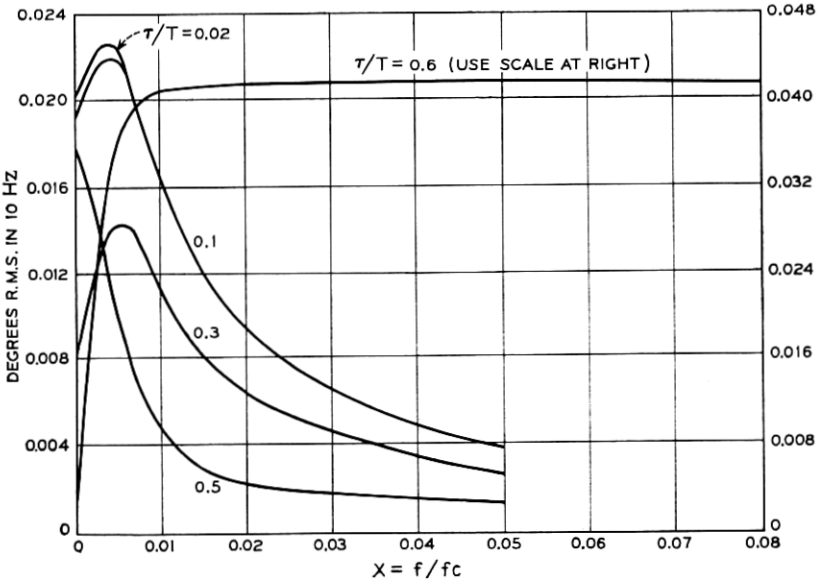

Fig. 20 — Calculated spectra of timing noise for several durations of rectangular pulses.

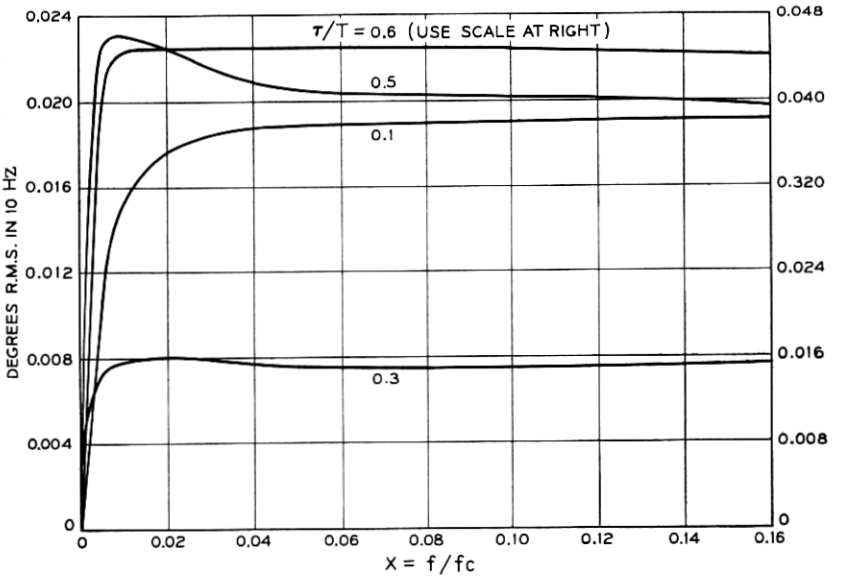

Fig. 21 — Calculated spectra of timing noise for rectangular pulses ($n = 1$ only).

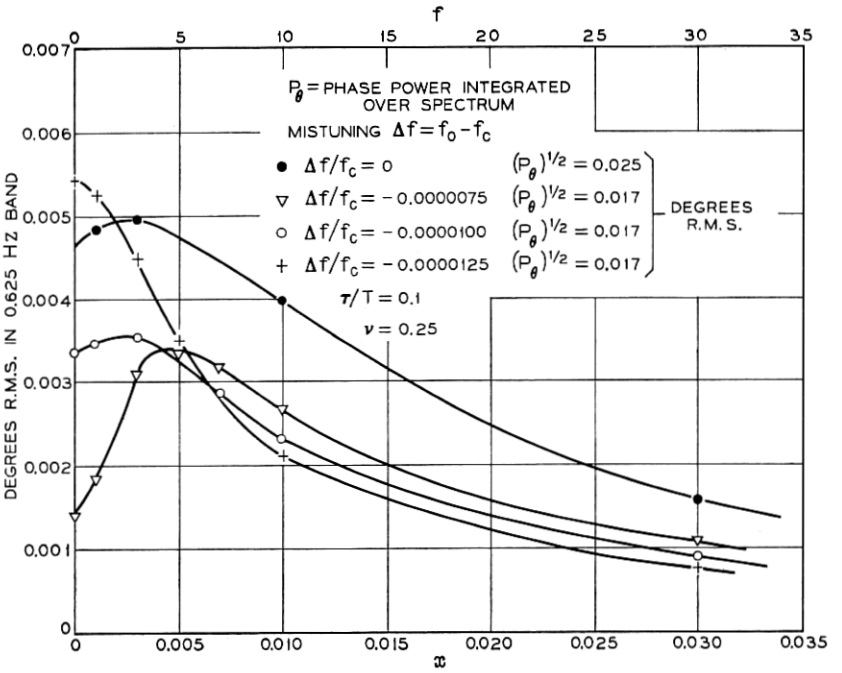

Fig. 22 — Spectrum of phase noise for rectangular pulse.

a single time slot and so the relations (108), (109), (110) hold. Here

$$F_2(t') = F_4(t') = 1 - \cos(2\pi t/T) \tag{115}$$

and

$$\frac{S(nf_c + f)}{S(f_c)} = -\frac{2}{\pi}\frac{\exp(j2\pi\nu x)\exp[j2\pi\nu(n-1)]\sin\pi(n+x)}{(n+x)[(n+x)^2-1]}. \tag{116}$$

The proper value of ν is 1/4.

The spectrum of timing noise is shown in Fig. 35, where it is seen that there is no noise energy at zero frequency. The pulse spectrum not only has nulls at all the pulse rate harmonics except the fundamental, but has very small energy in all the high frequencies. Thus, in this case, the high frequencies have very little effect on the timing noise. This was verified by both further calculation and measurement.

For x not too large, the noise spectrum is nearly

$$(w_\theta(f))^{\frac{1}{2}} \approx (T/2)^{\frac{1}{2}}\frac{\sin\pi x}{\pi}\frac{(9+16x^2Q^2)^{\frac{1}{2}}}{1+4x^2Q^2}\ \text{rad/Hz}. \tag{117}$$

2.6.5.3 *1.5T Raised Cosine Pulse.* This pulse shape is drawn in Fig. 23a. A single pulse is described by

$$f(t) = 1-\cos(4\pi t/3T). \tag{118}$$

Consideration of the specification (54) shows that

$$\left.\begin{aligned} F_2(t') - F_3(t') &= f(t') - f(t'+T) \\ F_4(t') &= f(t') + f(t'+T) \end{aligned}\right\} \quad 0 < t' < T/2$$
$$\left.\begin{aligned} F_2(t') - F_3(t') &= f(t') \\ F_4(t') &= f(t') \end{aligned}\right\} \quad T/2 < t' < T. \tag{119}$$

Thus, even though there is overlapping of adjacent pulses, $\delta_m = 0$ and the pulse spectrum is completely specified by S_m. Consideration of the waveform of Fig. 23(a) for all pulses present shows that $\nu = 1/2$ is the proper value here. S_m/S_N is independent of ν for this value and is

$$\frac{S_m}{S_N} = \exp(j\pi x)(-)^n \frac{5}{8}\frac{[1 - \exp(-j\pi m/N)]}{(m/N)(4/9 - m^2/N^2)} \cdot\left\{\frac{m^2}{N^2}[1 + \exp(-j\pi m/N)] + \frac{4}{9}\exp(j\pi m/N)\right\}. \tag{120}$$

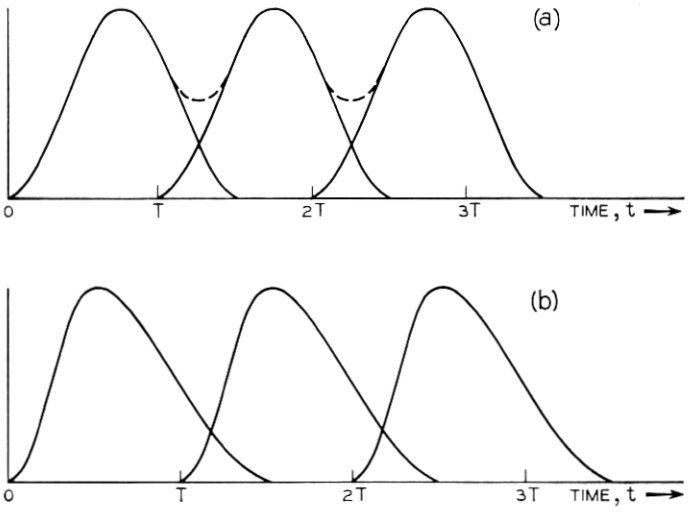

Fig. 23 — Pulse waveforms.

The spectra of timing noise, caused by this pulse shape, calculated and measured, are plotted in Fig. 36. While the magnitude (rms) of this noise is about 4 times that for $1T$ pulses, the energy at zero frequency is 0.00075 degree in a 10 Hz band, which is quite small. Hence overlapping of pulses does not appear to be a source of very low frequency timing noise. As in the previous case, the high frequency part of the response is small and so has only a small effect on the timing noise.

2.6.5.4 *Asymmetrical Overlapping Pulses.* The particular pulse shape chosen here is pictured in Fig. 23b, where it is seen that the rise occurs in one-half pulse period while the decline takes a whole period. The auxiliary function $F_2(t)$ is described by

$$\begin{aligned} F_2(t') &= 1 - \cos 2\pi t'/T && 0 < t' < T/2 \\ &= 1 - \cos \pi(t' + T/2)/T && T/2 < t' < 3T/2. \end{aligned} \tag{121}$$

From this and F_3 and F_4, it is found that the δ function is zero as in the previous case. The spectrum function S_m is

$$\frac{S_m}{S_N} = \frac{2j}{\pi} \frac{\exp(j2\pi x\nu) \exp[j2\pi\nu(n-1)]}{(1 - j4/3\pi)(n + x)} \cdot \left\{ \frac{1 + \exp[-j2\pi(n+x)]}{1 - 4(n+x)^2} - \frac{1 + \exp[j\pi(n+x)]}{1 - (n+x)^2} \right\}. \tag{122}$$

Estimates indicate that $\nu = 0.35$ will bring the zero crossing of the fundamental term very close to the sampling time of $t = 0$ and so this value was used in the calculations. The spectrum of timing noise caused by this pulse shape is plotted in Fig. 36, where it is seen that the amount at zero frequency is quite small, although somewhat larger than that of the symmetrical overlapping pulses. Hence, asymmetry of pulse shape does not appear to be a significant factor in very low frequency timing noise.

Since no readily available means for generating this pulse shape in the laboratory was found, there is no measured data. The good agreement between calculation and measurement in the other cases gives considerable weight to the calculated curve.

2.6.5.5 *Rectified 2T Raised Cosine Pulses.* Rectified $2T$ raised cosine pulses are pictured in Figs. 17 and 18. Before rectification, a single pulse occupying two time slots is represented by

$$f_2(t) = 1 + \cos(\omega_c/2)t \qquad -T < t < T \tag{123}$$

where $f_c = \omega_c/2\pi$ is the pulse rate. After rectification, the auxiliary functions are shown in Fig. 17c and described by

$$\begin{aligned} F_2(t') &= 0, && 0 \leqq t' \leqq T/2 \\ &= -\cos(\pi t'/T), && T/2 \leqq t' \leqq T \\ F_3(t') &= \cos(\pi t'/T), && 0 \leqq t' \leqq T/2 \\ &= 0, && T/2 \leqq t' \leqq T \\ F_4(t') &= 1, && 0 \leqq t' \leqq T. \end{aligned} \tag{124}$$

Because of the nonlinearity, the δ function is not zero. The pulse spectrum is described by

$$\begin{aligned} S_m &= \frac{1}{\pi} \frac{\exp[-j(3\pi/2)(m/N)] \cos(\pi m/N) \sin(\pi m/N)}{(m/N)(1 - 4m^2/N^2)} \\ \delta_m &= \frac{1}{\pi} \frac{\exp[-j(3\pi/2)(m/N)][\sin(\pi m/N) - 2m/N]}{(m/N)(1 - 4m^2/N^2)} \end{aligned} \tag{125}$$

$$S_N = 0, \quad \delta_N = j2/3\pi, \quad \langle C_N \rangle_{av} = j/6\pi \text{ for } \nu = 1/4, \quad p = 1/2.$$

The spectrum of timing noise calculated from (125) is plotted in Fig. 37. The sums in (107) were carried to 15 terms, but the higher order terms added very little. The results are very close to those for $n = 1$ except at zero frequency. The higher frequency terms with aliasing do generate some noise at these. The amount, which is difficult to see in the Fig. 37, is 0.0023 degree rms in a 10 Hz band, about three times that for $1.5T$ pulses and one-half that for the asymmetrical pulses.

2.6.6 *Relation of the General Theory to the Simpler One*

The operation $U_+ - U_-^*$ which appears in (92) for the calculation of phase deviation is essentially the same as the operation used in Section 2.2 for determining symmetrical and antisymmetrical components or in phase and quadrature components. The expression $U_+ - U_-^*$ is

$$U_+ - U_-^* = (S_+/\langle C_N \rangle_{av})(Y_+/Y_N) - (S_-/\langle C_N \rangle_{av})^*(Y_-/Y_N)^*. \tag{126}$$

In the simpler derivations of Section 2.2, it was assumed that the pulse train was such that $(S_+/\langle C_N \rangle_{av}) = (S_-/\langle C_N \rangle_{av})^*$ and so could

be factored out leaving

$$U_+ - U^*_- = (S/\langle C_N\rangle_{av})[Y_+/Y_N - (Y_-/Y_N)^*]. \quad (127)$$

Or, in other words, the pulse train contributed to the phase deviation in magnitude only. The part within the brackets is the conversion factor caused by mistuning, if any, in the tuned circuit described by Y. In the case of the offset trigger, a separate conversion factor was derived.

The simple theory cannot be applied generally for the wider pulses and particularly in those cases when the δ function enters into the pulse spectrum description. In some cases considered in detail, it was found that the strength of noise components σ_m (and hence the dissymmetry between side frequency pairs about the pulse rate) depends largely on the δ_m part of (79), and very little on the S_m part, while the situation is just the reverse for the phase deviation ϕ_k in (92).

III. SYSTEM USED FOR MEASUREMENTS

3.1 *Principal Apparatus*

In Fig. 24, the connection diagram of Fig. 1 has been revised to show the detection and remodulation process. This also shows why the actual apparatus used (bottom diagram) is really parts of two repeaters.

The complete block diagram of the apparatus used, corresponding to the simplified diagram at the bottom of Fig. 24 is shown in Fig. 25. The functioning of this apparatus will now be described in more detail. The principal sections are:

3.1.1 *Pulse Regenerator*

The pulse regenerator has been especially developed so that it will not add any timing noise of its own. It was worked out mainly by C. R. Crue following plans made by S. L. Freeny. To make the first record (simulating repeater 1), the regenerator input is switched to the source of clipped random noise, thus generating a random train of pulses. Thereafter it is switched to the recorder playback so that the same sequence of pulses, though random, is used for each transmission through the apparatus. A fixed bias may also be connected to the regenerator input so that it sends an all pulses present train to the system for calibration and testing.

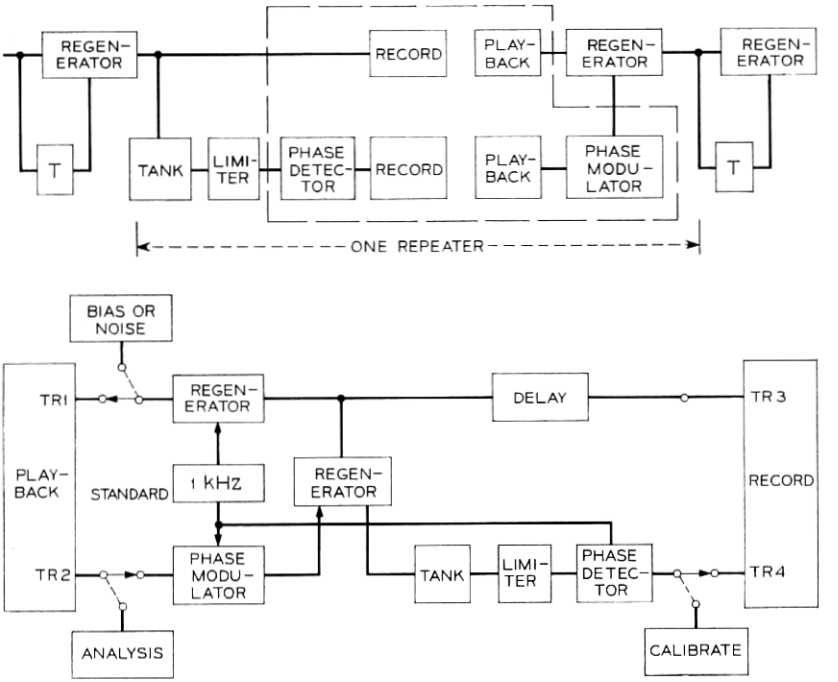

Fig. 24 — Block diagram of simulation of chain of regenerative repeaters. Part within dashed section at top is redrawn at bottom.

3.1.2 *LC Tank Circuit*

The LC tank circuit which derives the timing wave from the incoming pulse train uses an air core coil and positive feedback to achieve a Q of 100. It is necessary to use an air core coil and to keep it in a temperature controlled oven in order to measure phase with the required precision of less than 0.1°.

3.1.3 *Amplitude Limiter*

A very important section and one which is difficult to achieve is the amplitude limiter which removes very nearly all the amplitude variation from the timing wave so that in the detection process, only the phase deviation of the timing wave is measured. For most of the measurements, the limiter has two stages, each consisting of amplifier, cathode follower, and series limiter made up of resistance and a pair

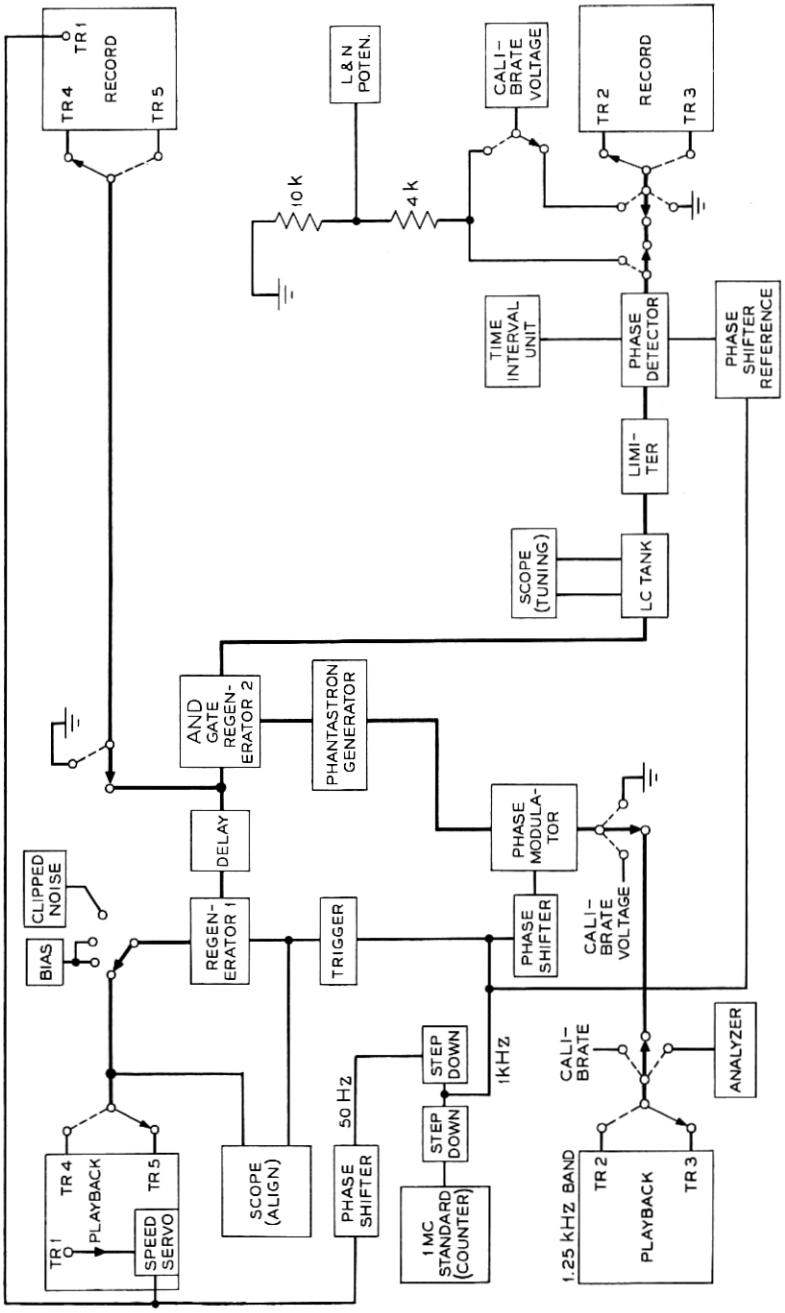

Fig. 25 — Detailed block diagram of system used for simulation of chain of regenerative repeaters. Heavy lines show signal paths.

of diodes. The amplifiers were made to approach linearity very closely and are isolated from the limiters by cathode followers in order to make amplitude to phase conversion negligible.

3.1.4 *Phase Detector Characteristic*

The phase detector characteristic, volts versus phase, extends through zero equally in both directions, and is linear over a wide range. How it works is explained briefly in the simplified diagram of Fig. 26. There are two inputs to the phase detector, the signal wave and the reference standard. At the positive zero crossings of these waves, sharp pulses are generated to operate the flip-flop whose output is the square wave at E when A and B are opposite in phase as shown. The edge of the square wave at E, controlled by the refer-

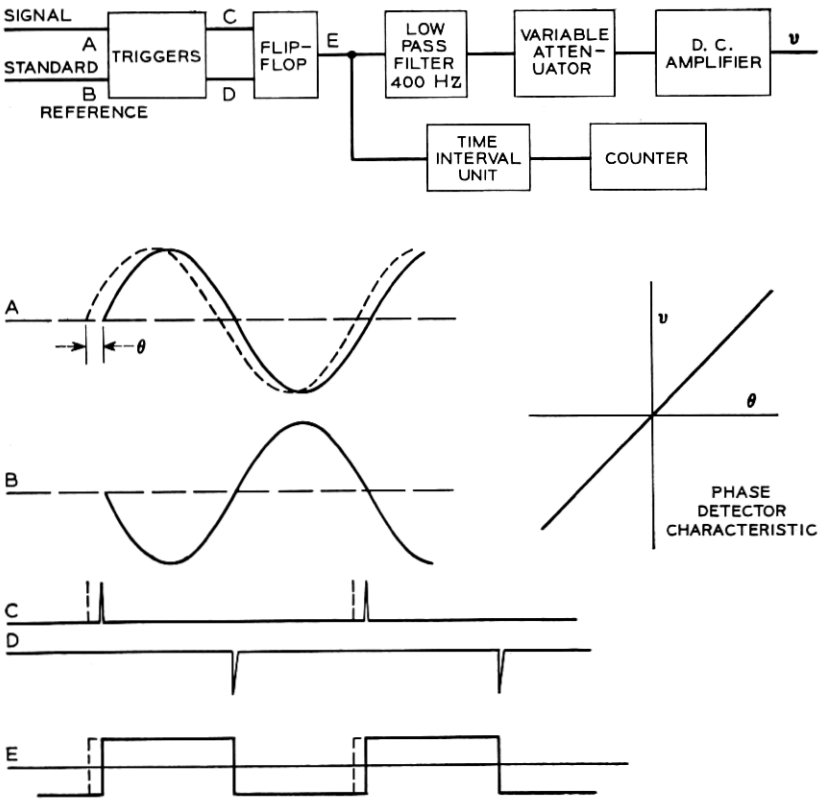

Fig. 26 — Block diagram and operation of phase detector.

ence standard, is fixed; the other edge varies as the phase of the signal wave. The average value of E appearing at the low-pass filter output is then proportional to the time variations of the positive zero crossings of the signal wave, that is, its phase. The low-pass filter and a little shaping in the dc amplifier are such that the bandwidth available for the detector output as indicated in Fig. 26 is about 0.4 the pulse rate. The noise wave thus derived is nearly the best continuous representation of the zero crossing deviations.

Since part of this detector is like a sampler operating at 1 kHz, there will be aliasing in the process if the original time variations contain frequency components higher than 0.5 kHz, as discussed in Section 2.6.4 and 2.6.5.

With the time interval unit and counter connected at E, the time duration from a fixed edge of the square wave to the adjacent variable edge can be measured so that individual zero crossing variations as well as the smoothed wave v may be obtained from the detector; or the time interval unit may be operated to measure from one variable edge to the next. In this way "spacing jitter" may be measured.

This connection is also used in the standardization of the detector characteristic. With an all pulses present train applied to the tuned circuit, a steady sine wave is obtained at the signal point A of the phase detector. The precision phase shifter which supplies the reference at point B is adjusted until the duration of the positive part of E is 500.0 microseconds. Then a bias adjustment is made to bring v to zero volts. After this the phase shifter is moved by various amounts from this reference condition and the amplifier gain adjusted to give the proper detector output voltage. In this calibration a Leeds and Northrup potentiometer is used for voltage measurement.

3.1.5 *Phase Modulator*

The phase modulator generates a sharp pulse at the instant voltage coincidence occurs between the input signal wave and a very "linear sawtooth" wave generated from the 1 kHz standard. This pulse is then used in the regenerator for timing the new pulses. The modulator must generate this timing pulse just as precisely as the phase detector detects the zero crossings of the original timing wave. It is calibrated by applying a known voltage which then causes a phase shift throughout the system. This phase shift is then converted to a voltage by the phase detector and the result compared with the input. The modulator sensitivity is adjusted so that the detector output is the same as the modulator input. Thus all calibration of the detection and

modulation process is in terms of two absolute standards, the Leeds and Northrup potentiometer for voltages and the phase shifter for phase angles.

The circuit for the modulator was originally developed and worked out by L. R. Wrathall. This was revised somewhat and built in final form and thoroughly tested by C. R. Crue.

3.1.6 *Tape Recorder*

The tape recorder used is an Ampex FR-100B with servo speed control such that reproduced signal time never varies by more than ±0.25 ms (1 ms = 1 pulse period) from precise time. Because the noise wave is essentially a low frequency signal with most of its energy below 5 Hz, and because frequency modulation (FM) recording is used, these small variations in time will affect only the time at which this old noise is added to the new. Tests have demonstrated that whatever time variation there is has a negligible effect. FM recording at 30 inches per second is used on five tracks, one of which is for speed servo. The machine is operated at 50 Hz derived by step-down chain from the 1 kHz standard which in turn is derived from the 1 MHz crystal oscillator in the counter. Two tracks provide a 5 kHz band for the pulse train. The other two tracks are for the phase noise signal and the bandwidth for these has been reduced to 1.25 kHz to lessen recorder noise. The gain through these channels is made unity. A phase shifter in the 50 Hz supply to the recorder makes it possible to align the recorded pulses with the gating triggers at the regenerator input each time the recorder is started.

3.1.7 *Delay Network*

The delay network in the pulse path makes up for the delays in the noise path caused mainly by the detection and recording process so that the noise record and pulse record correspond at any time.

3.1.8 *Trigger Circuit and Envelope Detector*

A trigger circuit with adjustable triggering level was introduced into the system in place of the limiter for the investigation of amplitude to phase conversion effects. Operation and data taking were simplified by removing the limiter entirely even though in a real repeater some limiting, though imperfect, would be used.

For the measurement of the properties of amplitude variations of the tuned circuit response, an envelope detector was connected at the tuned circuit output.

3.1.9 *Pulse Shaping Networks*

For the study of wide pulses and intersymbol interference, pulse shaping networks were introduced between the pulse regenerator and the tank circuit. These were RC circuits and low-pass filters for producing a sine-squared shape. In some cases a half-wave rectifier was introduced between filter and tank circuit.

3.1.10 *Longword Pulse Pattern*

In order to investigate some aspects of timing noise, an attachment to the signal generator was made so that a longword pulse pattern with a period of 240 bits, and hence having important components within the band of the tank circuit, could be applied to the system. The basic parts of this attachment are (*i*) a code plate with a rectangular 15 by 16 array of holes, placed before (*ii*) a cathode ray tube, the electron beam of which is swept across all the holes successively, and (*iii*) a light sensitive device to convert the light coming through the code plate holes into pulses. The longword signal pattern which is desired is then brought about by blocking out with black tape the proper holes in the code plate. This apparatus was developed by C. R. Crue.

3.2 *Method of Operating the System*

In using the system to obtain a series of noise records corresponding to the timing noise at successive repeaters in a chain, the procedure is as follows. After calibrations have been made with the all pulses present condition, the regenerator is connected to the clipped noise source (which has been adjusted to give the desired pulse density) and recordings are made of the pulse train on track 5, the generated phase noise in the timing wave on track 3, and the 50 Hz servo control wave on track 1, for about 15 minutes. Then the tape is rereeled, calibration checked, and playback started with track 3 going to the phase modulator and track 5 going to the pulse regenerator. This time the pulse train is recorded on track 4 and the timing noise on track 2. We now have two timing noise records corresponding to the timing waves at the first and second repeaters of a chain and these are now analyzed following the procedure outlined below.

Notice that it is the phase noise on the timing wave which is analyzed here rather than the repeater output pulses. These are the same, of course, in a completely retimed repeater. Therefore, it is not necessary that the recorded pulse train have the accumulated

timing noise; it is a perfectly timed replica of the original pulse train. The first part of the regenerator removes any time variations acquired in the recording-playback process. In the first recording, a few minutes of all pulses present is recorded before switching to the random train to give the recorder servo time to synchronize and also to allow time for the alignment of recorder to system each time it is started.

To obtain the next pair of records corresponding to transmission through repeaters 3 and 4 of the chain, track 2 is played back to the phase modulator, while the detected accumulated noise is recorded on track 3 thus erasing the record first made there. Then track 3 is played back to the modulator with the new noise record being made on track 2. And so on, as long as desired or until some difficulty in the process arises.

During the playback, the alignment of system and recorder is monitored continuously to make sure that the recorder stays in synchronism. If it does not, the pulse train may be altered.

A great amount of time and effort has gone into the building of the system just described to make it sufficiently stable and accurate for measuring phase deviations to within less than 0.1° out of 10°. It is necessary to measure with this precision in order to be able to describe accurately the change in noise from one repeater to the next because of the small amounts involved. The rms value of noise generated at one repeater with $Q = 100$ and 0.1 percent detuning is a little less than 1°.

Another factor in the reliability of the data is that a long enough signal was used for analyzing so that fluctuations in the plotted parameters of the noise were fairly small. As described below, 32 ten-second averages of the time the noise wave spends below each threshold are used for each point on the cumulative distributions. Since the counter rests for 10 seconds after each adding period, the length of signal involved is 640,000 pulse positions. Each plotted point is well enough established, so that the curve connecting them is smooth without the necessity of further averaging.

The residual noise at the detector output for all pulses present is about 0.006° rms. For a random train of pulses (narrow) there should be no phase noise generated if the tank circuit is centered exactly on the pulse rate. In this situation, the residual noise is about 0.012° rms. See Fig. 28. This is not only a good test of the system as a whole, but is a good dynamic test of the limiter, which is hard to do in any other way.

3.3 *Apparatus for and Process of Analyzing Data*

3.3.1 *Cumulative Distribution-Slicer Circuit*

To obtain the cumulative distribution of the noise, a slicer circuit was developed. This is an adjustable threshold device which generates a standard height pulse whenever the noise wave is below the threshold. The duration of each of these pulses is measured by counting the number of cycles of a 100 kHz wave which the pulse gates to the counter. The accumulated durations of all these pulses which occur in a standard interval of 10 seconds is then totaled by the counter.

At each threshold setting, 32 of these totals are obtained and plotted in control chart fashion as shown in Fig. 27. This helps us to see if the data are statistically acceptable. If appreciable trouble has occurred in the apparatus during the run, it will show up in this picture. The median taken from each chart of data is used to plot one point on the distribution. After the distribution is plotted, the rms value is taken from 1/3 the difference of the values at the 93.3

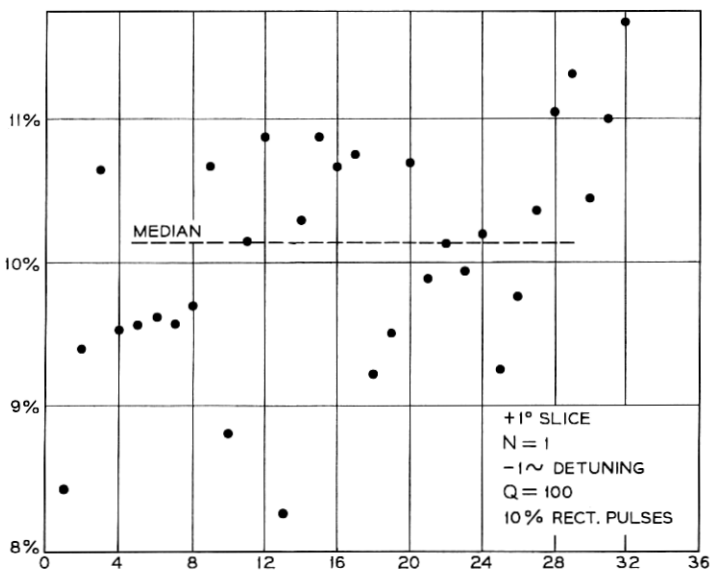

Fig. 27 — Control chart plot of data to obtain one point of cumulative distribution (as in Fig. 31) of timing noise amplitudes.

percent and 6.7 percent points, following a method suggested by E. B. Ferrell for skewed distributions.

3.3.2 *Spectrum Density—Wave Analyzer*

To obtain the spectrum density of the noise wave, a General Radio 1900A wave analyzer with external rms indicator is used. In order to extend the nominal 20 Hz lower end of the analyzer to around 1 Hz, a 16-to-1 speedup of the noise wave is made in a second recording process. Each point on the cumulative distribution requires about 11 minutes of signal, so the original noise record is played back and then rereeled for each point. During each playback the noise record is duplicated at lower speed by bridging the input of another FR-100 recorder operating at 1⅞ inches per second at the main recorder output. The new record then consists of about 8 to 10 serial duplications of the noise which, when played back at 30 inches per second, provides about 5 minutes total of the original noise with all frequency components multiplied by 16. A wave analyzer band of 10 Hz then is equivalent to a 0.625 Hz band for the original noise.

In order to obtain consistent and reliable measurements of noise power in the wave analyzer band, it was found necessary to replace the linear detector provided in the wave analyzer with a square law detector. To do this, the wave analyzer IF output was connected to a Ballantine rms meter and the square law response of this applied to a 4-second time constant RC smoothing circuit and a linear scale meter. The pointer of this meter still fluctuates, thus requiring some kind of average. This average was obtained arithmetically from 20 successive meter readings made at 5-second intervals and, after calibration, was taken as the measure of the mean square power of the noise falling within the wave analyzer band at each frequency setting.

The variance of each of these readings depends partly on the analyzing filter bandwidths and partly on the lengths of signal record available. The latter part could be obtained only by calculation and appears to be the dominating part. Variance estimated this way indicates that any reading taken by the above method is within 10 percent of the true value with 95 percent confidence. The data taken appear to have less variation than this. Some further smoothing of an unknown amount occurs in the plotting of the individual points to give a smooth spectrum curve. Integration of these curves consistently gave results agreeing (within a very few percent) with measurements of total noise power.

IV. RESULTS OF EXPERIMENTS

4.1 *Use of Narrow Rectangular Pulses*

The first measurements of phase noise on the timing wave recovered from a random train of narrow pulses by a tank circuit mistuned from the pulse rate showed that the magnitude of the noise is proportional to the amount of mistuning when this is only a few tenths of a percent, as predicted by W. R. Bennett.[1] Hence there should be no noise for zero mistuning. It was found difficult to define, though, just what zero mistuning is for a real LC tank circuit. In the experiments reported here, the tank circuit consisted of an air core coil and capacitor in shunt at the collector of a transistor, the emitter of which had a resistor equal to the resonant impedance of the LC tank. The transistor was driven at its base and there was positive feedback using another transistor to bring the effective Q of the tank to a value of 100. The reference point from which mistuning was measured, chosen because it could be easily set with sufficient precision, was that of 180° phase between the collector and emitter voltages of the tank transistor as determined by an oscilloscope Lissajou figure.

That the minimum of phase noise does not occur at this point is shown by the curve of Fig. 28. Neither is its value zero, being made up partly of the residual noise of the system as indicated by APP (for all pulses present) and partly of the noise from the train of random narrow rectangular pulses. However, in the investigation of noise caused by pulse shape alone (Section 4.3), it was found that this minimum does not coincide with zero mistuning. Rather, the minimum is the result of cancellation by small amounts of mistuning and trigger offset of part of the noise attributable to pulse shape. While the minimum is about 0.012 degree, the noise from the pulses is about 0.036 degree. This is the true zero mistuning and occurs about where the curve crosses this ordinate. Even though the noise contributed by the narrow rectangular pulses is not zero, it is quite small as may be seen from the spectrum curves of Figs. 4 and 20. Hence using the narrow rectangular pulses in the measuring of noise caused by tank circuit mistuning and by offset trigger gives results which very nearly isolates these as sources for individual scrutiny.

4.2 *Tank Circuit Mistuning*

The curves of Fig. 2 show how the spectrum changes as the noise is examined at successive repeaters, each mistuned by the same amount and direction, in a chain of six repeaters. Distinctive features of these

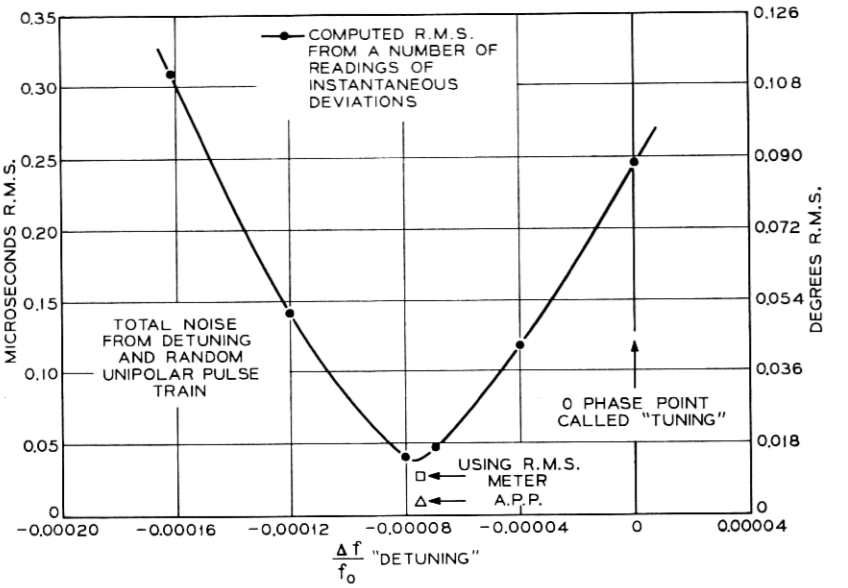

Fig. 28 — Measured timing noise as a function of tank circuit detuning near minimum. This shows residual noise of the system.

spectra are the zeros at zero frequency and the maxima which occurs at $f = f_o/2Q$ for $N = 1$ and closer to zero as N increases. Additional measurements on longer chains up to 20 in length show that this trend continues and agrees with magnitudes predicted by the theory presented in Section II. In Fig. 14, these predictions are plotted and extended to a chain of 100 repeaters. It is evident from these results that while the maximum continues to rise, its magnitude will never be greater than four times what it was at the first repeater. The reason for this is that the noise spectrum generated at each repeater is zero at zero frequency and the succeeding tank circuits continually attenuate the higher frequency components. These effects are seen also in the data on the total phase noise along the chain. For chains up to 20 in length, measured and calculated values are plotted in Fig. 29. Calculated values for longer chains are plotted in Fig. 15.

Figure 30 shows the measured and calculated spectra of phase noise at two adjacent repeaters when the second one is mistuned in the opposite direction but by the same amount as the first one. This has the effect of reversing the dissymmetry of side frequencies about the carrier in the second repeater, and so there is a partial canceling

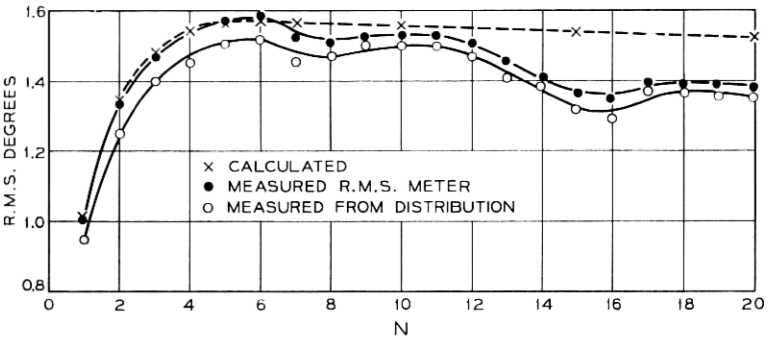

Fig. 29 — Total timing noise caused by 0.1 percent mistuning of timing tanks in chains of N like regenerative repeaters.

of phase noise. Thus the greatest accumulation of timing noise caused by mistuning comes when all repeaters in a chain are mistuned the same way.

In all these cases, we have seen how well the values of timing noise calculated from the theoretical model of Section II agree with those

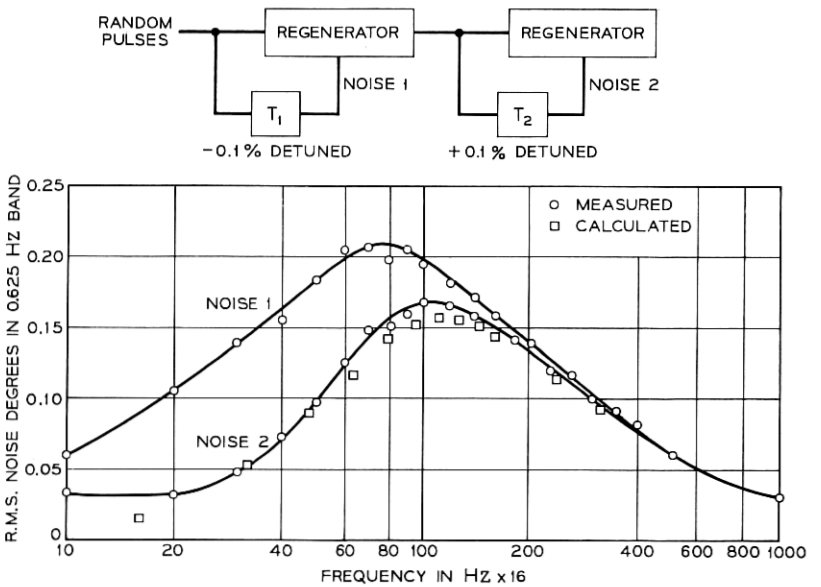

Fig. 30 — Spectra of timing noise at two successive regenerative repeaters with oppositely detuned timing tanks.

obtained by measurement. The theoretical model was developed from the simple picture of the equivalence of phase modulation of the recovered carrier and dissymmetry of the side frequencies about this carrier introduced by the mistuning of the tank circuit into the otherwise symmetrical side frequency and carrier representation of the random pulse train.

The cumulative distribution curve of phase noise generated at a mistuned repeater, obtained from measurements, is shown in Fig. 31 and is seen to have a shape which is approximately log-normal. Calculation of a distribution curve which agrees quite well with these results has been made by M. R. Aaron and J. R. Gray.[9] When the distributions of timing noise at successive repeaters along a chain are examined, it is found that the skewness is gradually reduced.

Another set of data from the measurements of timing noise caused by mistuning is that concerning spacing noise which is displayed in Fig. 32. Spacing noise is defined as the deviations from normal of the spacing between successive positive (or negative) going zero crossings of the timing wave. As suggested by M. R. Aaron and H. E.

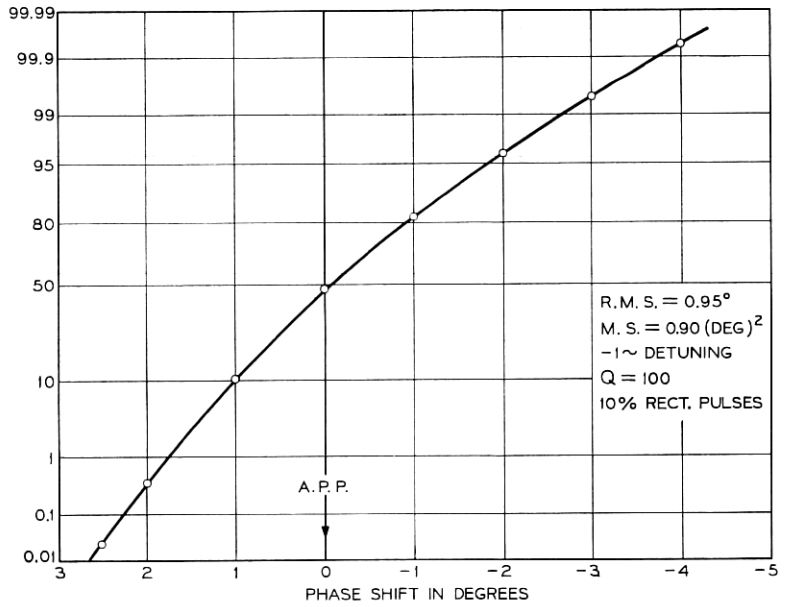

Fig. 31 — Cumulative distribution of timing noise amplitudes obtained from measurements (noise caused by tank detuning).

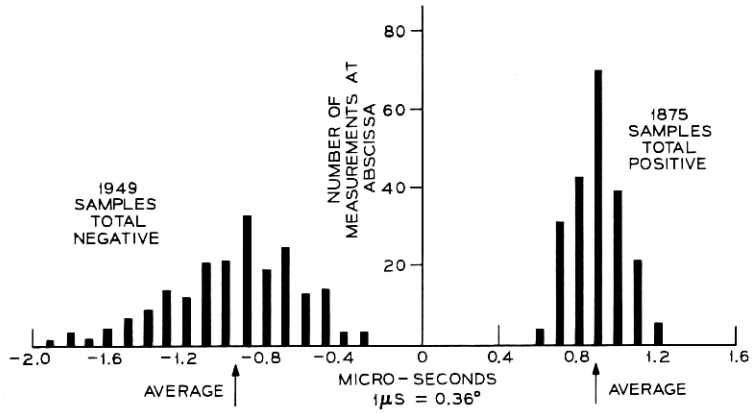

Fig. 32 — Timing wave spacing noise caused by tank mistuning. Measured deviations of zero-crossing differences from 1.0 millisecond.

Rowe, the reason for this lies in the quantized character of changes in the pulse pattern. That is, at any point in time, the next time slot has either a pulse or no pulse. The magnitudes can be found from the results shown in Fig. 39a for one absent pulse in 240 and mistuning. Scaling this to 0.1 percent mistuning (condition for Fig. 32), gives a peak phase change of 0.36° or 1 μs. For a single pulse added, the phase change would have the opposite sign. Since the most likely change in the random pulse train is that of a single pulse added or left out and other changes are less likely, the distribution of Fig. 32 should have peaks near $+1$ μs and -1 μs as observed.

4.3 *Amplitude-to-Phase Conversion*

The pulse rate fundamental recovered from the signal pulse train by narrowband tank circuit has appreciable phase deviations only if the tank circuit is mistuned from the pulse rate. But this fundamental has noisy amplitude variations even when the tank circuit is perfectly tuned.

By connecting an envelope detector at the tank circuit output, recordings were made of the response amplitude variations. The spectrum is shown in Fig. 33 where it is seen to have a nonzero value as frequency approaches zero as predicted by the calculated values superimposed and as also shown by the calculated curve of Fig. 8. That this must be so may be seen by considering that the noise side frequencies continue to exist at about the same magnitude as they

get closer to the carrier (pulse rate). That is, the amplitude modulation is not reduced, only the dissymmetry disappears. The measured cumulative distribution of the amplitude variations is very nearly normal.

One way in which these amplitude variations may be converted into phase variations is through an imperfection in the trigger circuit which, from the timing wave, generates sharp pulses for retiming the signal pulses. Such will be the case if the triggering level of this circuit is, for some reason, offset from the zeros of the timing wave.

This kind of timing noise was generated in the system for simulating a chain of regenerative repeaters by replacing the amplitude limiter which follows the tank circuit in Fig. 9 with a trigger circuit having an adjustable threshold. In a real repeater, some amplitude limiting, though imperfect, would be used between tank and trigger, but here it is more convenient to leave out all limiting.

Spectra of this amplitude to phase timing noise, when there is no mistuning, at successive-like repeaters in a chain of six are plotted in Fig. 3 along with calculated points. The spectra have the same shape as that of the amplitude variations since the two phenomena are directly related. The rms magnitudes at very low frequencies

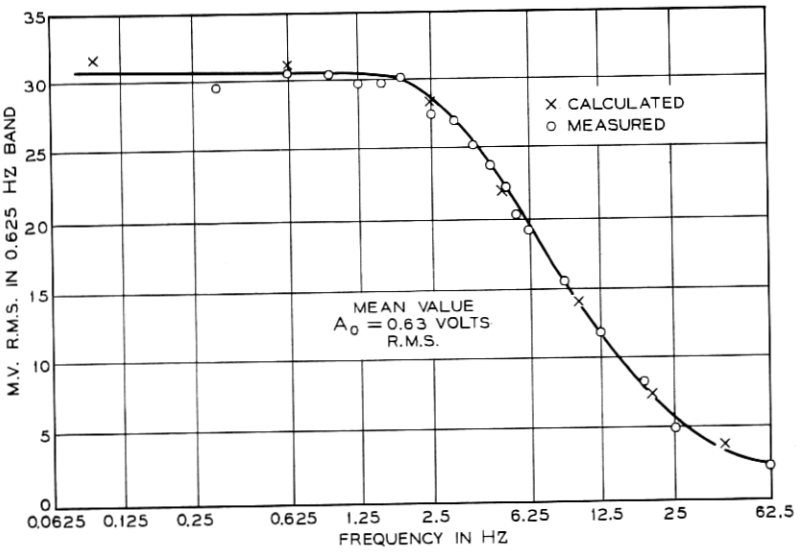

Fig. 33 — Spectrum of amplitude variation of tuned circuit response to random unipolar rectangular pulses.

grow directly with repeater number because of the nonzero magnitude of noise and nearly zero tank circuit attenuation at very low frequencies. Total timing noise in the same situation is shown in Fig. 34. The cumulative distribution of the noise is somewhat curved, about like the amplitude to phase conversion characteristic of the trigger circuit.

Timing noise was measured also when mistuning and amplitude to phase conversion were both present in the same repeater. This is shown in Fig. 10, along with calculated values.

We see in all these results very good agreement between the measured values and those calculated, as outlined in Section II, by the method developed first in the investigation of noise caused by mistuning.

4.4 *Phase Noise Attributable to Pulse Form*

4.4.1 *Rectangular Pulses*

After it was found that the low sharp minimum of timing noise shown in the curve of Fig. 28 was attained by small deviations from zero mistuning and zero trigger offset, fairly good agreement between measured and calculated noise spectra for rectangular pulses was obtained. Most of the curves of Fig. 4 are from measurements while those of Figs. 20 and 21 are from calculations.

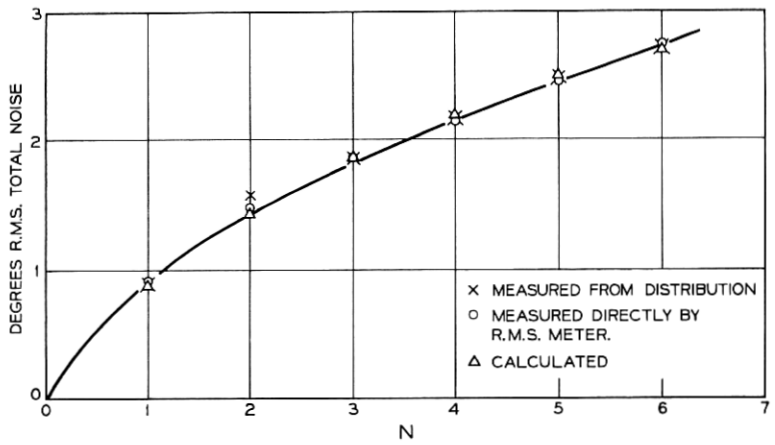

Fig. 34 — Total timing noise from amplitude variation of timing wave and offset trigger as a function of the number (N) of repeaters in a chain.

It is only the narrow rectangular pulses which have the magnitude and shape of noise spectrum which can be changed to produce the result of Fig. 28 by small adjustments of the two indicated factors. The calculated curves of Fig. 22 show how this can be. For rectangular pulses with $\tau/T = 0.6$, the total noise changes only about 10 percent as the tuning varies over the range of Fig. 22.

An attempt was made to measure the effect of high frequencies in the tank circuit response by cutting out these components; it was not entirely satisfactory because of the difficulty of obtaining a suitable filter. The results were sufficient though to verify the general features of the differences between the curves of Fig. 20 and Fig. 21.

4.4.2 *Raised Cosine Pulses*

Trains of pulses approximating the raised-cosine shape were generated by applying the 10 percent duty factor rectangular pulses to a 4-section low-pass filter built from a design by W. E. Thomson.[12] Filters were built to generate pulses $1T$, $1.5T$, and $2T$ wide at their bases. Oscilloscope presentations of the $1T$ pulses are shown in Fig. 18c and of the $2T$ pulses in Fig. 18a.

The measured spectrum of phase noise caused by the $1T$ pulses is shown in Fig. 35 along with the calculated values and it is seen that agreement is fairly good. This spectrum has appreciable energy at considerably higher frequencies than does that caused by mistuning or trigger offset and narrow rectangular pulses. The reason for this is that the dissymmetry of side frequencies extends to much higher frequencies. The same is true of course for the rectangular pulses wider than $\tau/T = 0.5$.

Measured and calculated spectra for the $1.5T$ pulses are plotted in Fig. 36 where it may be seen that the total amount of noise is about four times as great as that for the $1T$ pulses.

Since there seemed to be no suitable way to generate the asymmetrical pulses, no experimental data is available for this case.

Some of the data obtained with rectified $2T$ pulses are presented in Fig. 37. It is difficult to duplicate experimentally the idealized waveform of Fig. 17b assumed in the calculations of this case. For example the wiggles at the top of the real waveform Fig. 18a come from small departures from ideal of the pulse shapes, and the rectifier does not produce cusps at its cutoff point but rounded transitions as in Fig. 18b. The data plotted in Fig. 37 agrees fairly well with calculation, and it is believed to be reliable. But other data has been

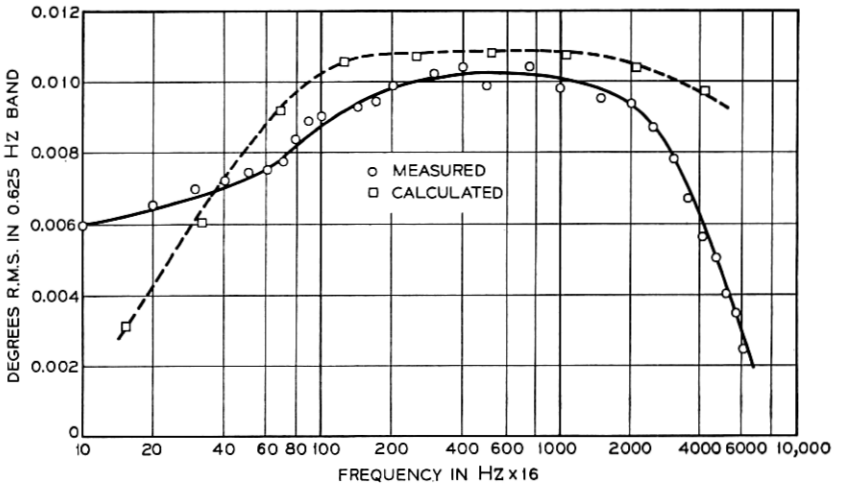

Fig. 35 — Spectrum of timing noise from raised cosine random pulses one time slot wide at base. No tank mistuning.

obtained which gives spectra both smaller and larger than that shown.

When the driving pulses are ac coupled to the shaping filter, there is a large increase in very low-frequency noise components as shown. This illustrates the statement made before that if there is low-frequency distortion in the transmission of pulses, then nonlinearity

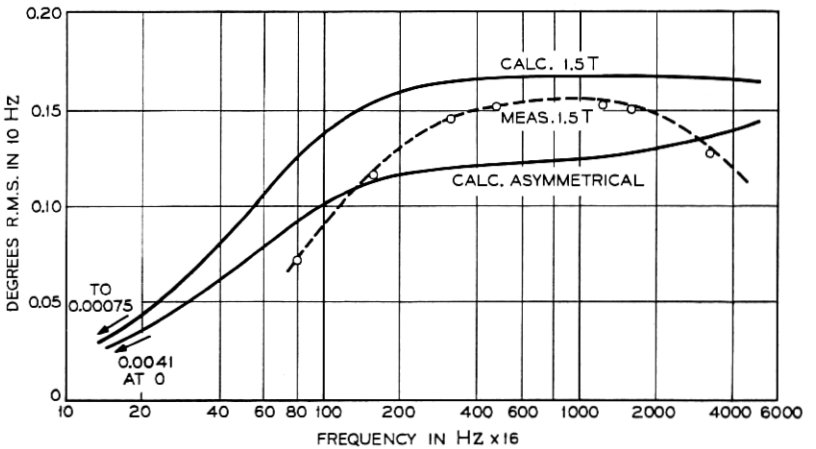

Fig. 36 — Timing noise spectra for 1.5 T and asymmetrical raised cosine pulses.

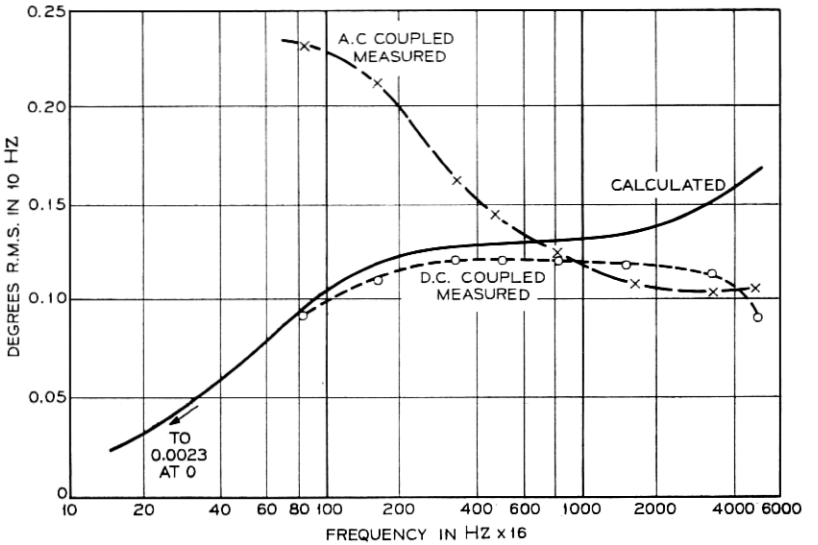

Fig. 37 — Spectrum of timing noise from rectified raised cosine puses two time slots wide. No tank mistuning.

which follows this can convert this distortion into very low-frequency phase noise. With ac coupling, the pulse waveform of Fig. 18(a) is changed to that of Fig. 38.

4.5 *Long Word Periodic Pulse Pattern*

In addition to the previous results obtained with a random pulse train, a few measurements were made using a periodic pulse pattern of period 240 time slots.

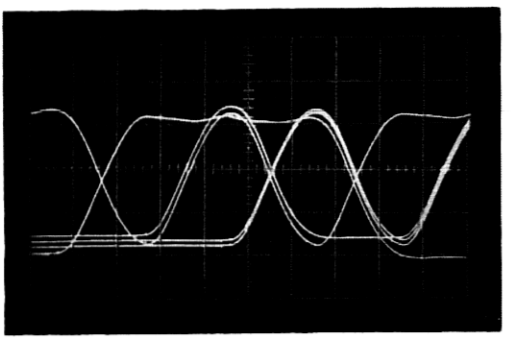

Fig. 38 — Photograph of random pulse oscilloscope traces for raised cosine pulses two time slots wide at base. AC coupling.

For a particular pattern chosen at random, the measured phase modulation on the recovered pulse rate agrees very closely with that calculated from the theory developed in Section II. Hence there is nothing in periodic pulse patterns as such to cause behavior different from that predicted by the theory.

Another particular pattern, with one pulse per period missing was used to measure a sort of phase impulse response. Under this condition phase deviation was observed and photographed under two conditions. Figure 39a shows the phase detector response for tank mistuning and Fig. 39b that for an offset trigger circuit following a perfectly tuned tank. In Fig. 39a, the mistuning is −0.2 percent and the peak phase deviation 0.73 degree. In Fig. 39b, the trigger offset is 12.6 degrees and the peak phase deviation is 0.43 degree. The wiggles on both waveforms are a residual noise in the system and have nothing to do with the phenomena being discussed.

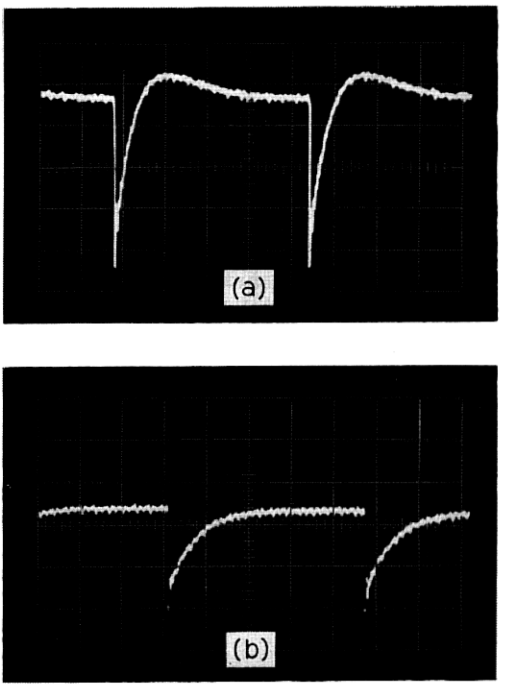

Fig. 39 — Photographs of oscilloscope traces—Phase deviation of recovered fundamental pulse rate for pattern of 239 pulses, 1 space, with (a) tank circuit mistuning, (b) amplitude to phase conversion by means of trigger offset.

Both of these resemble the response of an RC circuit to an impulse. A simple picture of this situation then is that deletion of one pulse from the all pulses present condition is converted, by one or the other of the two imperfections considered, into an equivalent impulse of phase change which through the tank phase transfer characteristic produces one of the responses of Fig. 39.

But there is a small, though significant, difference between the two responses. The simpler of the two, Fig. 39b, with its sharp rise and exponential decline is very close to an RC impulse response. Its measured time constant is about 30 ms which is quite close to the value of 32 ms which describes the phase transfer characteristic derived from sine-wave measurements. The Laplace transform of this pulse is $F(p) = 1/(p + \alpha)$. Its amplitude spectrum, with its finite value at zero frequency, is like the measured spectra of phase noise caused by amplitude to phase conversion.

The pulse in Fig. 39a differs from the other, principally in its crossing of the baseline and undershooting as it declines to zero. The observed pulse can be approximated very closely by the modified exponential $f_1(t) = e^{-\alpha t}(1 - \alpha t)$ which has the Laplace transform

$$F(p) = \frac{p}{(p + \alpha)^2}.$$

The corresponding amplitude spectrum is

$$| F(j\omega) | = \frac{| \omega |}{\omega^2 + \alpha^2}.$$

It is seen that $f_1(t)$ goes through zero at $t = t_0 = 1/\alpha$ and has a minimum value of $-e^{-2} = -0.135$ at $t - = 2t_0$. Also, it is seen that $| F(j\omega) |$ has its maximum at $\omega = \alpha$. From the photograph, we estimate that $t_0 = 33$ ms and that the minimum of 0.135 occurs at $2t_0$. Further, from the earlier work we find that both measurement and theory show a maximum in the spectrum of phase noise caused by tank circuit mistuning at $\omega = \omega_0/2Q$. Equating this to α gives $1/\alpha = 32$ ms which is very good agreement with the estimation of t_0 .

Thus the "impulse response" view of phase deviation in the fundamental recovered by means of a narrowband tank circuit is consistent with the spectrum modification view worked out earlier.

V. CONCLUSIONS

Two important sources of timing noise in a self-timed regenerative PCM repeater, namely tank circuit mistuning and amplitude to phase

conversion by means of an offset trigger circuit, have been identified and studied both experimentally and theoretically. Another source, pulse shape and duration has been studied less than the other two. Another subject investigated is the way these noises accumulate along a chain of repeaters and how they combine.

As a part of this investigation, a simple theoretical picture of the process has been developed whereby many important properties of timing noise and its accumulation along a chain of repeaters can be calculated with results which agree very well with corresponding measurements.

The process of calculation begins with the spectrum of the pulse train, then proceeds to the modifications of it which arise as the pulse train is transmitted through the timing tank and retiming process of each repeater. The properties of the timing noise which appear on the retiming wave depend on the particular character of these modifications. The further modifications of the spectrum of the pulse train, acquired at each repeater, are used to find the way in which the timing noise accumulates along the repeater chain.

These investigations have shown that the characters of the spectra of these timing noises are important in determining how they accumulate along a chain of repeaters. It has been found that the spectrum of the noise caused by tank circuit mistuning has a zero at zero frequency. It has been demonstrated that because of its property, the noise increases only for the first few repeaters of the chain, soon reaching a limit. Further, it has been found that the spectrum of timing noise which depends on amplitude variations of the timing wave (as in a trigger circuit where the firing point has been offset from a zero crossing) has a nonzero value at zero frequency. It has been shown that because of this property, this timing noise increases without limit along the repeater chain. The total amount of the noise varies inversely with the Q of the tank circuit.

Thus, whether or not timing noise increases without limit along a repeater chain depends, not on whether the same noise is generated and added on at each repeater, but on whether or not the spectrum of the noise added at each repeater has a nonzero value at zero frequency.

Study of the effect of pulse shape and duration have shown that while the total noise from this source is greater than it is for the others, the amount at very low frequencies is quite small, though not zero in a number of cases. These latter components are the result of aliasing of the high-frequency parts of the tank circuit response.

If there is nonlinearity in the fundamental recovery path, low-frequency pulse distortion during transmission can be converted to very low frequency timing noise.

VI. ACKNOWLEDGMENTS

S. L. Freeny has had an active part in this project during much of the time it was carried on. Also, consultation with him has been frequent and valuable. The work of C. R. Crue in developing and building and testing quite a bit of the apparatus used was very helpful. Many helpful conversations with S. O. Rice, and the analysis carried out by him for the case of wide overlapping pulses, are gratefully acknowledged. Numerous consultations with B. G. King and J. A. Young, who supervised the work during much of the time, were very valuable in bringing the project to a successful conclusion.

REFERENCES

1. Bennett, W. R., "Statistics of Regenerative Digital Transmission," B.S.T.J., *37*, No. 6 (November 1958), pp. 1501–1542.
2. Wrathall, L. R., "Transistoried Binary Pulse Regenerator," B.S.T.J., *35*, No. 5 (September 1956), pp. 1059–1084.
3. Sunde, E. D., "Self-Timing Regenerative Repeaters," B.S.T.J., *36*, No. 4 (July 1957), pp. 891–938.
4. DeLange, O. E., "The Timing of High-Speed Regenerative Repeaters," B.S.T.J., *37*, No. 6 (November 1958), pp. 1455–1486.
5. DeLange, O. E. and Pusetlnyk, M., "Experiments on the Timing of Regenerative Repeaters," B.S.T.J., *37*, No. 6 (November 1958), pp. 1487–1500.
6. Rowe, H. E., "Timing in a Long Chain of Regenerative Binary Repeaters," B.S.T.J., *37*, No. 6 (November 1958), pp. 1543–1598.
7. Aaron, M. R., "PCM Transmission in the Exchange Plant," B.S.T.J., *41*, No. 1 (January 1962), pp. 99–141.
8. Byrne, C. J., Karafin, B. J., and Robinson, D. B., "Systematic Jitter in a Chain of Digital Regenerators," B.S.T.J., *42*, No. 6 (November 1963), pp. 2679–2714.
9. Aaron, M. R. and Gray, J. R., "Probability Distribution for the Phase Jitter in Self-Timed Reconstructive Repeaters for PCM," B.S.T.J., *41*, No. 2 (March 1962), pp. 503–558.
10. Kinariwala, B. K., "Timing Errors in a Chain of Regenerative Repeaters, I and II," B.S.T.J., *41*, No. 9 (November 1962), pp. 1769–1797.
11. Kinariwala, B. K., "Timing Errors in a Chain of Regenerative Repeaters, III," B.S.T.J., *43*, No. 4 (July 1964), pp. 1481–1504.
12. Thomson, W. E., "The Synthesis of a Network to Have a Sine-Squared Impulse Response," Inst. of Elec. Eng. Proc. (London), *99*, part III (November 1952), pp. 373–376.